

## Preferential N–H···C< Hydrogen Bonding Involving Ditopic NH-Containing Systems and N-Heterocyclic Carbenes

Zacharias J. Kinney,<sup>[a]</sup> Arnold L. Rheingold,<sup>[b]</sup> and John D. Protasiewicz<sup>[a]\*</sup>

Electronic Supporting Information

\*email: protasiewicz@case.edu

1)	Experimental Procedures	2
2)	NMR Spectra	4
3)	<sup>1</sup> H NMR Comparison of Parent Amines to Adducts	29
4)	Evaluation of DPA···IPr Hydrogen Bond Strength	32
5)	Crystallographic Analysis	34
6)	References	38

## 1) Experimental Procedures

Reactions were carried out under an inert atmosphere of nitrogen via an MBraun glovebox or traditional Schlenk line techniques. Unless otherwise noted, all starting materials, reagents, and solvents were purchased from commercial sources and used without further purification. Anhydrous solvents (THF, hexanes, toluene) were purified using a MBraun solvent purification system equipped with alumina column. THF-*d*<sub>8</sub> and C<sub>6</sub>D<sub>6</sub> were distilled over sodium. (**IPr**)<sup>1</sup>, 3,3'-bicarbazole (**BC**)<sup>2</sup>, 3-(4,4,5,5-tetramethyl-1,3,2-dioxaborolan-2-yl)-carbazole<sup>3,4</sup> were prepared in accordance to the literature with minimal modification. NMR spectra were measured on a Bruker Avance III 500 MHz spectrometer, with all samples referenced to the residual solvent signal.

### **BC···2IPr** Adduct

**BC** (0.093 mmol) was massed into a 6-dram vial and dissolved in 2 mL THF. **IPr** (0.186 mmol) was massed into a separate vial and dissolved in 2 mL THF. The **IPr** solution was transferred to the vial containing **BC** solution. The **IPr** vial was rinsed with 1 mL fresh THF and added to the reaction mixture (5 mL THF total). Reaction vial was sealed, shaken vigorously to ensure that all solids were dissolved, then allowed to stand for 30 minutes. Once complete, volatiles were removed *in vacuo*, yielding **BC···2IPr** in quantitative yield as an off-white solid. Vapor diffusion of hexanes into a solution of **BC···2IPr** in THF resulted in pale yellow crystals suitable for X-ray diffraction. <sup>1</sup>H NMR (500 MHz, THF-*d*<sub>8</sub>) δ = 11.91 (s, 2H), 8.21 (d, J=1.8, 2H), 8.00 (d, J=6.9, 2H), 7.51 (t, J=7.8, 4H), 7.42 (dd, J=8.4, 1.8, 2H), 7.37 (d, J=7.8, 8H), 7.31 (s, 4H), 7.05 (ddd, J=8.2, 7.1, 1.3, 2H), 6.99 (td, J=7.4, 1.1, 2H), 6.59 (d, J=8.4, 2H), 6.54 (d, J=8.1, 2H), 2.87 (hept, J=7.0, 8H), 1.23 (d, J=7.0, 24H), 1.13 (d, J=6.9, 24H). <sup>13</sup>C{<sup>1</sup>H} NMR (126 MHz, THF-*d*<sub>8</sub>) δ 215.2, 147.2, 142.1, 140.5, 139.3, 134.2, 129.8, 125.8, 125.7, 124.6, 124.5, 124.4, 123.1, 120.6, 118.8, 118.7, 111.8, 111.7, 29.5, 25.0, 23.9

### **DPB···2IPr** Adduct

**DPB** (0.252 mmol) was massed into a 6-dram vial and dissolved in 5 mL THF. **IPr** (0.507 mmol) was massed into a separate vial and dissolved in 3 mL THF. The **IPr** solution was transferred to the vial containing **DPB** solution. The **IPr** vial was rinsed with 2 mL fresh THF and added to the reaction mixture (10 mL THF total). Reaction vial was sealed, shaken vigorously to ensure that all solids were dissolved, then allowed to stand for 30 minutes. Once complete, volatiles were removed *in vacuo*, yielding **DPB···2IPr** in quantitative yield as an off-white solid. Due to the inherently weak nature of the adduct, purification and crystallization were not feasible. <sup>1</sup>H NMR (500 MHz, THF-*d*<sub>8</sub>) δ = 7.54 (s, 2H), 7.42 – 7.34 (m, 8H), 7.27 (d, J=7.7, 8H), 7.19 (s, 4H), 7.15 – 7.09 (m, 3H), 7.01 (d, J=8.6, 4H), 6.98 (d, J=7.3, 3H), 6.75 (t, J=7.3, 1H), 2.82 (hept, J=6.9, 8H), 1.20 (d, J=6.9, 24H), 1.15 (d, J=6.9, 24H). <sup>13</sup>C{<sup>1</sup>H} NMR (126 MHz, THF-*d*<sub>8</sub>) δ 220.1, 146.9, 145.2, 143.6, 139.7, 133.9, 129.9, 129.4, 127.7, 124.2, 122.7, 120.6, 118.6, 118.1, 29.4, 25.0, 23.9

### **DPPD···2IPr** Adduct

**DPPD** (0.164 mmol) was massed into a 6-dram vial and dissolved in 5 mL THF. **IPr** (0.328 mmol) was massed into a separate vial and dissolved in 3 mL THF. The **IPr** solution was transferred to the vial containing **DPPD** solution. The **IPr** vial was rinsed with 2 mL fresh THF and added to the reaction mixture (10 mL THF total). Reaction vial was sealed, shaken vigorously to ensure that all solids were dissolved, then allowed to stand for 30 minutes. Once complete, volatiles were removed *in vacuo*, yielding **DPPD···2IPr** in quantitative yield as a brown solid. Crude material was dissolved in THF:Hexanes (2 mL: 3 mL) and stored at -35 °C, resulting in brown crystals suitable for X-ray diffraction after 3 days. <sup>1</sup>H NMR (500 MHz, THF-*d*<sub>8</sub>) δ = 7.36 (t, J=7.7, 4H), 7.26 (d, J=7.7, 8H), 7.21 – 7.17 (m, 6H), 7.11 – 7.03 (m, 4H), 6.90 (s, 4H), 6.86 (d, J=7.9, 4H), 6.66 (t, J=7.3, 2H), 2.82 (hept, J=6.9, 8H), 1.19 (d, J=7.0, 24H), 1.15 (d, J=6.9, 24H). <sup>13</sup>C{<sup>1</sup>H} NMR (126 MHz, THF-*d*<sub>8</sub>) δ 220.3, 146.9, 146.7, 139.7, 138.3, 129.8, 129.4, 124.1, 122.7, 121.3, 119.4, 116.5, 29.4, 25.0, 23.9

### **DPA···IPr** Adduct

**DPA** (1.42 mmol) was massed into a 50 mL Schlenk flask and dissolved in 10 mL THF. **IPr** (1.42 mmol) was massed into a 6-dram vial and dissolved in 5 mL THF. The **IPr** solution was transferred to the Schlenk flask containing **DPA** solution. The **IPr** vial was rinsed with 5 mL fresh THF and added to the reaction mixture (20 mL THF total). Reaction flask was sealed and stirred vigorously for 30 minutes. Once complete, volatiles were removed *in vacuo*, yielding **DPA···IPr** in quantitative yield as a white solid. A saturated solution in toluene was stored at -35 °C, resulting in colorless crystals. <sup>1</sup>H NMR (500 MHz, C<sub>6</sub>D<sub>6</sub>) δ = 7.31 (t, J=7.7, 2H), 7.19 (d, J=7.7, 4H), 7.04 (dd, J=8.8, 7.0, 4H), 6.88 – 6.74 (m, 6H), 6.60 (s, 2H), 6.27 (s, 1H), 2.93 (hept, J=6.9, 4H), 1.25 (d, J=6.9, 12H), 1.17 (d, J=6.9, 12H). <sup>13</sup>C{<sup>1</sup>H} NMR (126 MHz, C<sub>6</sub>D<sub>6</sub>) δ 218.2, 146.3, 144.1, 138.8, 129.4, 129.2, 123.8, 121.7, 120.6, 118.2, 28.8, 24.7, 23.7

#### 4-(carbazol-3-yl)-*N*-phenylaniline, **CD**

Under inert atmosphere a 100 mL Schlenk flask was charged with 3-(4,4,5,5-tetramethyl-1,3,2-dioxaborolan-2-yl)-carbazole (2.29 mmol), 4-bromodiphenylamine (2.30 mmol),  $\text{Cs}_2\text{CO}_3$  (4.59 mmol),  $\text{Pd}(\text{PPh}_3)_4$  (0.11 mmol), and toluene (18 mL). Reaction flask was transferred to manifold and placed under inert atmosphere. Under positive pressure degassed EtOH (4 mL) was added, and flask was equipped with a reflux condenser. Reaction temperature was brought to 85 °C and stirred for 16 hours. Reaction was cooled to RT, quenched with  $\text{H}_2\text{O}$  (50 mL), extracted with EtOAc (3 x 25 mL), washed with brine, dried over  $\text{MgSO}_4$ , filtered, and concentrated to yield **CD** as a crude brown solid. Purification via flash column with toluene as eluent affords pure product as a white solid, 422.9 mg (55%).  $^1\text{H}$  NMR (500 MHz, THF- $d_8$ )  $\delta$  = 10.25 (s, 1H), 8.29 (d,  $J$ =1.8, 1H), 8.10 (d,  $J$ =7.8, 1H), 7.63 (d,  $J$ =1.8, 1H), 7.60 (d,  $J$ =8.5, 2H), 7.44 (d,  $J$ =8.4, 1H), 7.40 (d,  $J$ =8.1, 1H), 7.36 (s, 1H), 7.35 – 7.29 (m, 1H), 7.22 – 7.18 (m, 3H), 7.19 – 7.16 (m, 1H), 7.15 – 7.11 (m, 2H), 7.12 – 7.09 (m, 1H), 6.84 – 6.78 (m, 1H).  $^{13}\text{C}\{^1\text{H}\}$  NMR (126 MHz, THF- $d_8$ )  $\delta$  145.3, 143.4, 141.9, 140.4, 135.5, 133.3, 130.0, 128.5, 126.4, 125.4, 124.9, 124.6, 121.0, 120.7, 119.6, 118.8, 118.6, 117.9, 111.7, 111.6

#### **CD**···**2IPr** Adduct

**CD** (0.172 mmol) was massed into a 6-dram vial and dissolved in 5 mL THF. **IPr** (0.345 mmol) was massed into a separate vial and dissolved in 3 mL THF. The **IPr** solution was transferred to the vial containing **CD** solution. The **IPr** vial was rinsed with 2 mL fresh THF and added to the reaction mixture (10 mL THF total). Reaction vial was sealed, shaken vigorously to ensure that all solids were dissolved, then allowed to stand for 30 minutes. Once complete, volatiles were removed *in vacuo*, yielding **CD**···**2IPr** in quantitative yield as an off-white solid. Due to the inherently weak nature of the adduct, purification and crystallization were not feasible.  $^1\text{H}$  NMR (500 MHz, THF- $d_8$ )  $\delta$  = 12.16 (s, 1H), 8.13 (d,  $J$ =1.8, 1H), 7.95 (d,  $J$ =6.4, 1H), 7.50 (d,  $J$ =8.6, 2H), 7.46 (t,  $J$ =7.8, 4H), 7.43 (s, 1H), 7.33 (d,  $J$ =7.8, 8H), 7.30 (dd,  $J$ =8.4, 1.8, 1H), 7.27 (s, 4H), 7.20 – 7.12 (m, 2H), 7.10 (d,  $J$ =8.6, 2H), 7.06 – 7.00 (m, 3H), 6.97 (t,  $J$ =7.4, 1H), 6.76 (t,  $J$ =7.3, 1H), 6.44 (d,  $J$ =8.6, 1H), 6.41 (d,  $J$ =7.8, 1H), 2.85 (hept,  $J$ =6.9, 8H), 1.22 (d,  $J$ =7.0, 24H), 1.14 (d,  $J$ =6.9, 24H).  $^{13}\text{C}\{^1\text{H}\}$  NMR (126 MHz, THF- $d_8$ )  $\delta$  217.3, 147.1, 145.5, 143.1, 142.1, 140.7, 139.5, 135.8, 132.5, 129.9, 129.7, 128.4, 125.7, 124.8, 124.6, 124.4, 124.3, 122.9, 120.4, 120.4, 119.0, 118.7, 118.0, 117.8, 111.8, 29.5, 25.1, 23.8

#### **CD**···**IPr** Adduct

**CD** (0.217 mmol) was massed into a 6-dram vial and dissolved in 5 mL THF. **IPr** (0.218 mmol) was massed into a separate vial and dissolved in 3 mL THF. The **IPr** solution was transferred to the vial containing **CD** solution. The **IPr** vial was rinsed with 2 mL fresh THF and added to the reaction mixture (10 mL THF total). Reaction vial was sealed, shaken vigorously to ensure that all solids were dissolved, then allowed to stand for 30 minutes. Once complete, volatiles were removed *in vacuo*, yielding **CD**···**IPr** in quantitative yield as an off-white solid. Due to the inherently weak nature of the adduct, purification and crystallization were not feasible.  $^1\text{H}$  NMR (500 MHz, THF- $d_8$ )  $\delta$  = 11.38 (s, 1H), 8.18 (d,  $J$ =1.8, 1H), 7.99 (d,  $J$ =7.7, 1H), 7.53 (d,  $J$ =8.5, 2H), 7.47 (t,  $J$ =7.7, 2H), 7.41 (dd,  $J$ =8.4, 1.8, 1H), 7.38 (s, 1H), 7.34 (d,  $J$ =7.7, 4H), 7.28 (s, 2H), 7.21 – 7.15 (m, 2H), 7.14 – 7.12 (m, 2H), 7.13 – 7.10 (m, 1H), 7.06 (d,  $J$ =7.4, 2H), 7.02 (t,  $J$ =7.6, 1H), 6.80 – 6.77 (m, 1H), 6.78 – 6.74 (m, 1H), 2.85 (hept,  $J$ =7.0, 4H), 1.22 (d,  $J$ =7.0, 12H), 1.12 (d,  $J$ =6.8, 12H).  $^{13}\text{C}\{^1\text{H}\}$  NMR (126 MHz, THF- $d_8$ )  $\delta$  216.4, 147.2, 145.4, 143.2, 142.0, 140.6, 139.4, 135.7, 132.8, 129.9, 129.7, 128.5, 126.0, 125.0, 124.7, 124.4, 124.4, 123.0, 120.6, 120.5, 119.0, 118.9, 118.2, 117.8, 111.8, 29.5, 25.0, 23.9

## 2) NMR Spectra

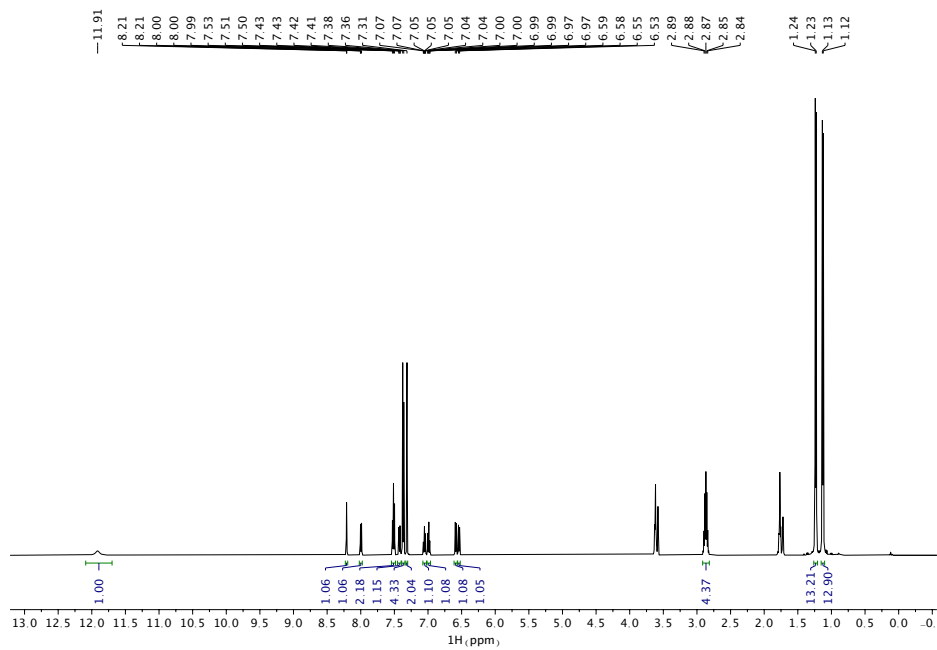


Figure 1.  $^1\text{H}$  NMR spectrum of **BC**···**2IPr** (50 mM, THF- $d_8$ , 500 MHz, 298 K)

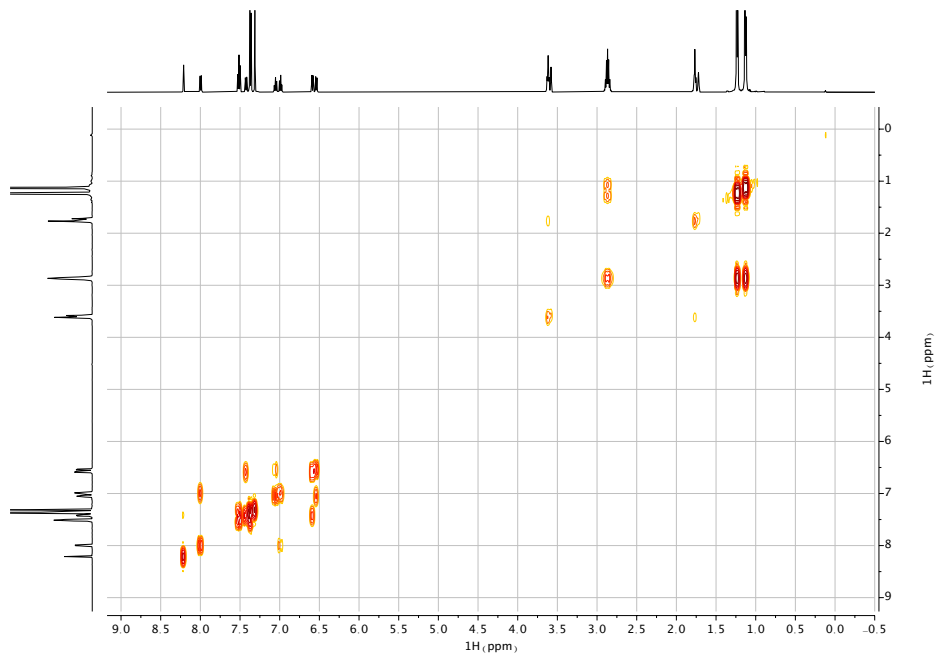


Figure 2.  $^1\text{H}$ - $^1\text{H}$  COSY spectrum of **BC** $\cdots$ **2IPr** (50 mM, THF- $d_8$ , 500 MHz, 298 K)

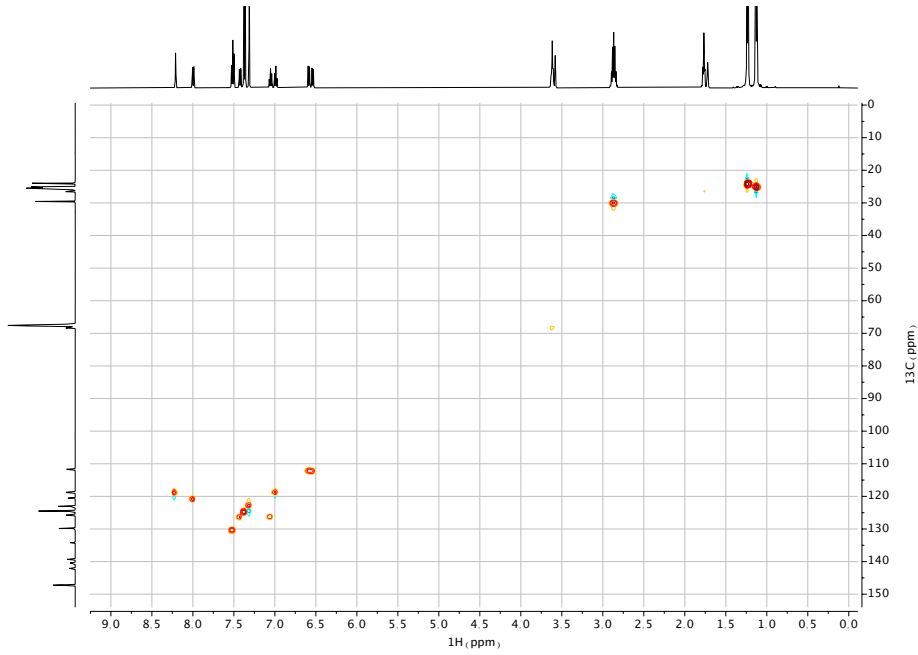


Figure 3.  $^1\text{H}$ - $^{13}\text{C}$  HSQC spectrum of **BC···2IPr** (50 mM, THF- $d_8$ , 500 MHz, 298 K)

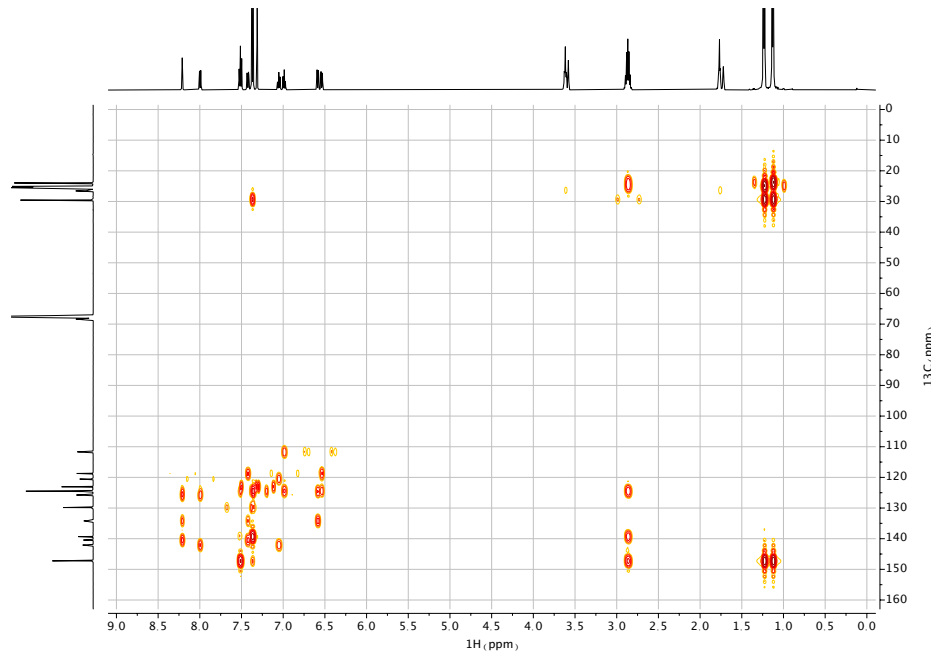


Figure 4.  $^1\text{H}$ - $^{13}\text{C}$  HMBC spectrum of **BC···2IPr** (50 mM, THF- $d_8$ , 500 MHz, 298 K)

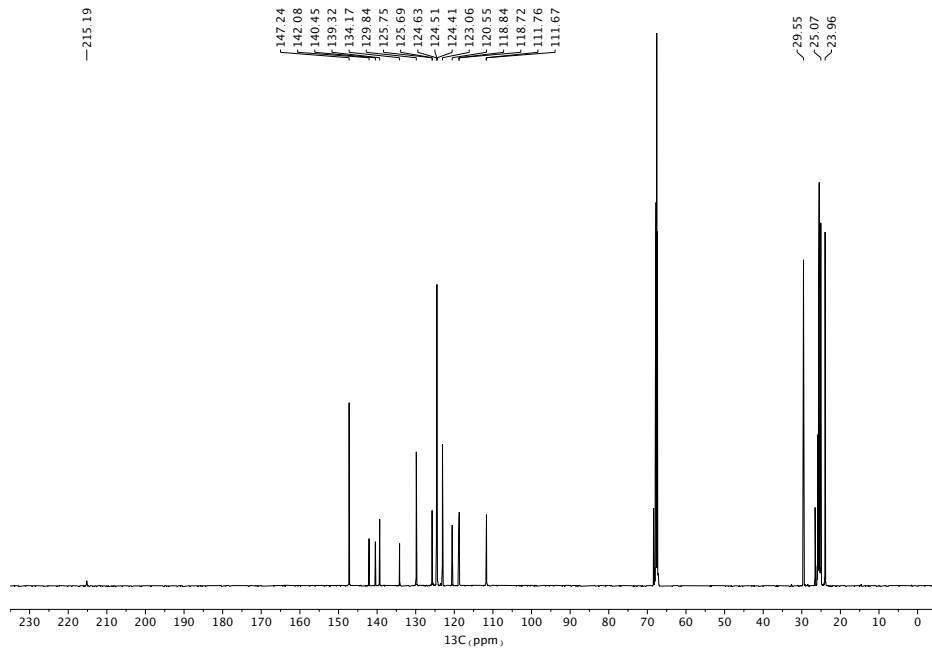
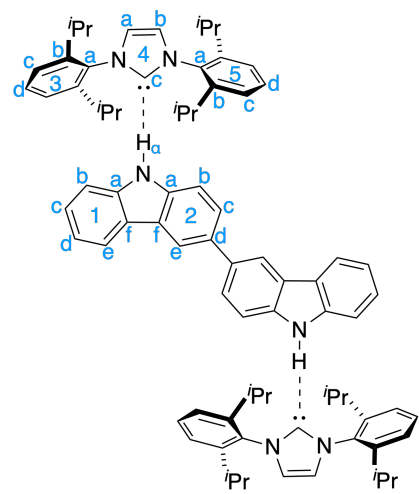


Figure 5.  $^{13}\text{C}\{^1\text{H}\}$  NMR spectrum of **BC**···**2IPr** (50 mM, THF- $d_8$ , 126 MHz, 298 K)



Assignment	$^1\text{H}$ δ	$^{13}\text{C}$ δ
H <sub>a</sub>	11.91	-
1a	-	142.1
1b	6.54	111.7*
1c	7.05	125.8*
1d	6.99	118.7*
1e	8.00	120.6
1f	-	124.4
2a	-	140.5
2b	6.59	111.8*
2c	7.42	125.7*
2d	-	134.2
2e	8.21	118.8*
2f	-	124.6
3a	-	139.3
3b	-	147.2
3c	7.37	124.5
3d	7.51	129.8
4a	7.31	123.1
4b	7.31	123.1
4c	-	215.2
5a	-	139.3
5b	-	147.2
5c	7.37	124.5
5d	7.51	129.8
i-Pr(CH)	2.85	29.5
i-Pr(CH <sub>3</sub> )	1.14 / 1.22	25.0 / 23.9

Figure 6. BC···2IPr with assignment of  $^1\text{H}$  and  $^{13}\text{C}$  resonances,  $^{13}\text{C}$  signals labelled \* are indistinguishable.

**DPB···2*i*Pr**

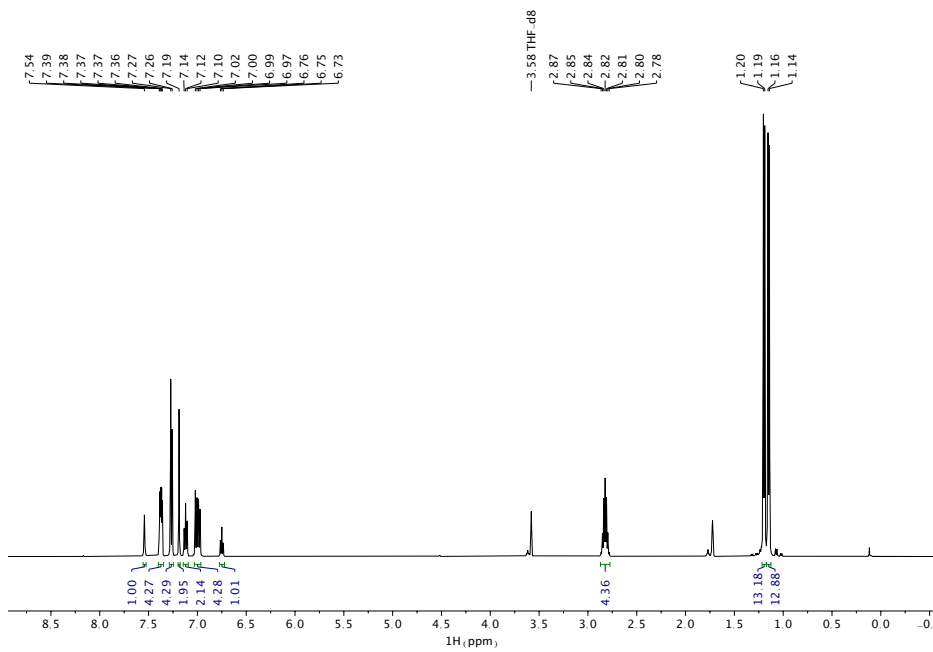


Figure 7. <sup>1</sup>H NMR spectrum of **DPB···2*i*Pr** (50 mM, THF-*d*<sub>8</sub>, 500 MHz, 298 K)

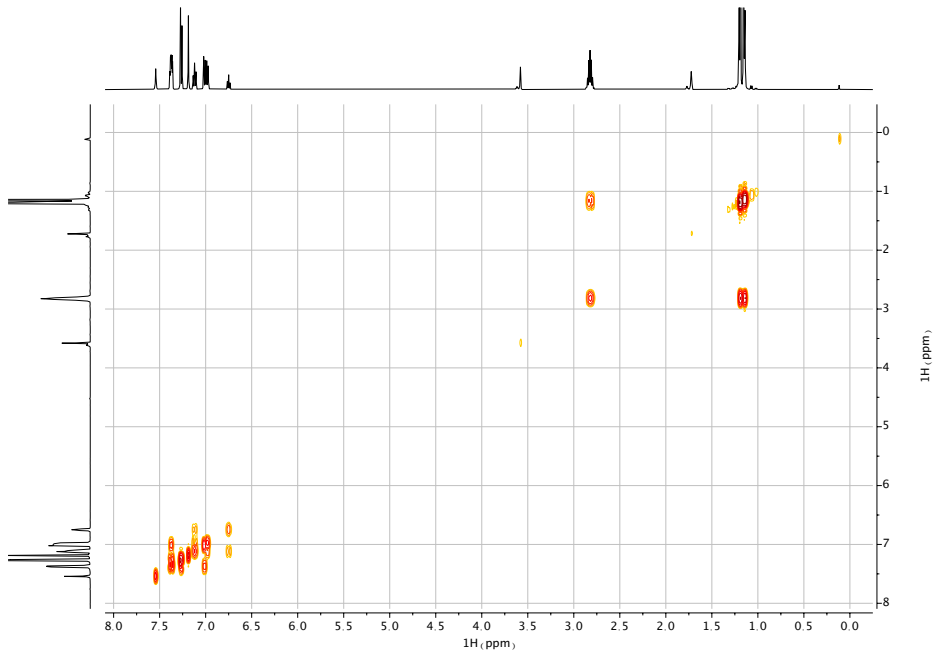


Figure 8. <sup>1</sup>H-<sup>1</sup>H COSY spectrum of **DPB···2*i*Pr** (50 mM, THF-*d*<sub>8</sub>, 500 MHz, 298 K)

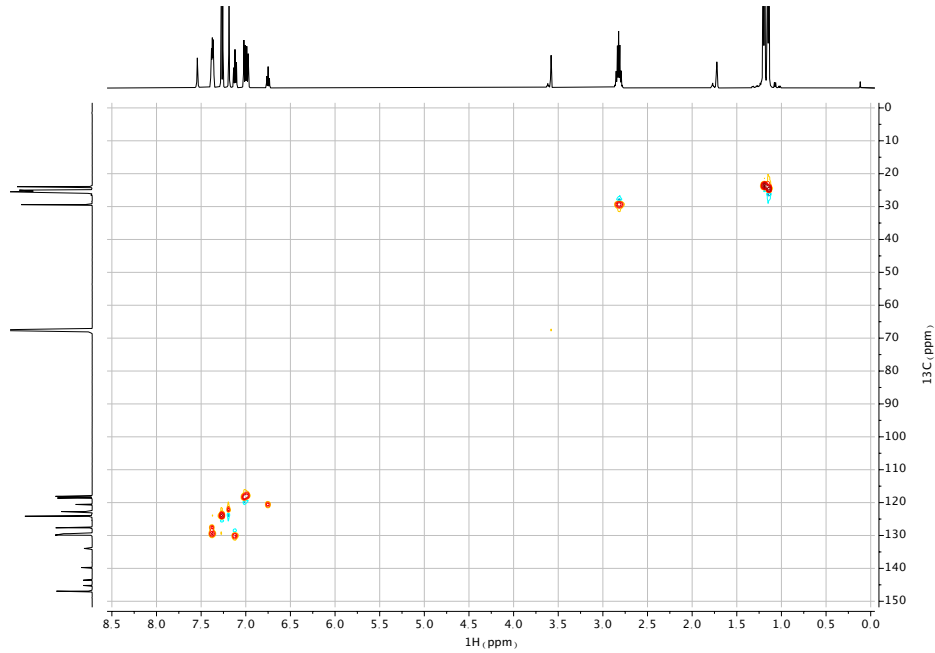


Figure 9.  $^1\text{H}$ - $^{13}\text{C}$  HSQC spectrum of **DPB···2IPr** (50 mM, THF- $d_8$ , 500 MHz, 298 K)

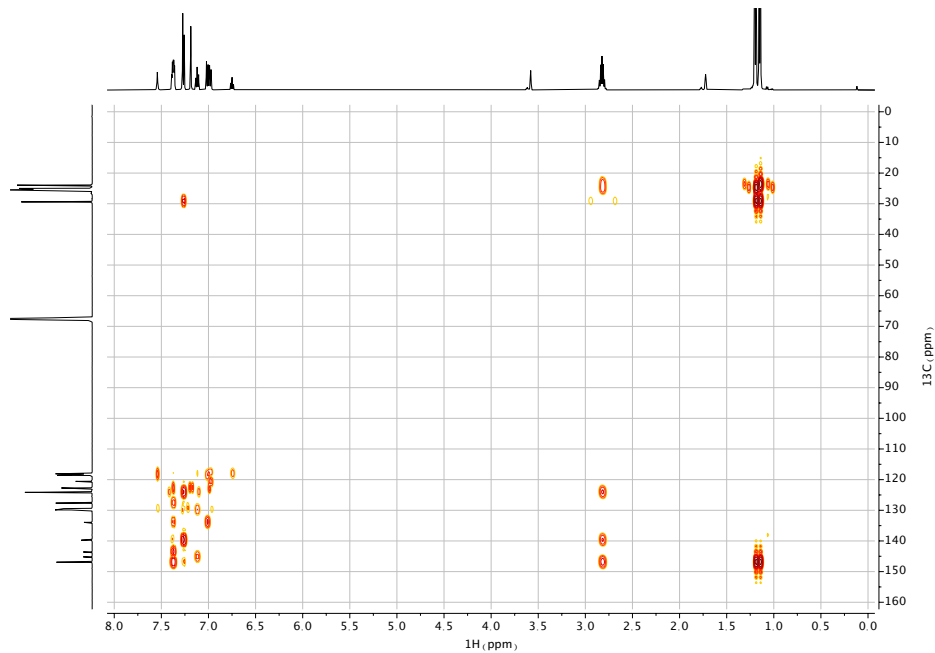


Figure 10.  $^1\text{H}$ - $^{13}\text{C}$  HMBC spectrum of **DPB···2IPr** (50 mM, THF- $d_8$ , 500 MHz, 298 K)

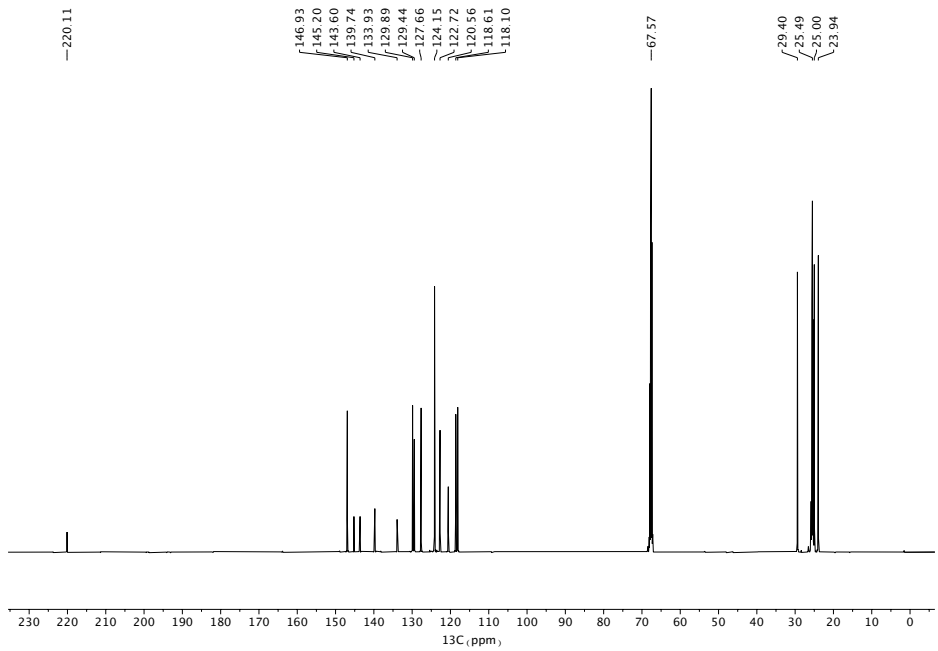
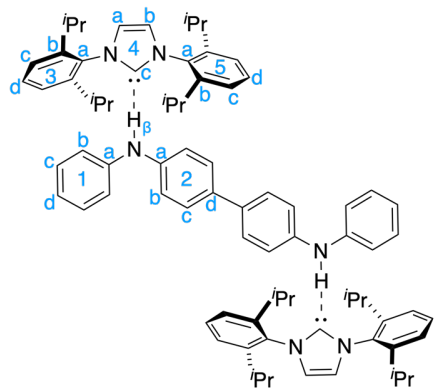


Figure 11.  $^{13}\text{C}\{\text{H}\}$  NMR spectrum of **DPB-2IPr** (50 mM, THF- $d_8$ , 126 MHz, 298 K)



Assignment	$^1\text{H } \delta$	$^{13}\text{C } \delta$
1a	-	145.2
1b	6.98	118.1
1c	7.12	129.9
1d	6.75	120.6
2a	-	143.6
2b	7.01	118.6
2c	7.36	127.7
2d	-	133.9
$\text{H}_\beta$	7.54	-
3a	-	139.7
3b	-	146.9
3c	7.27	124.2
3d	7.38	127.7
4a	7.19	122.7
4b	7.19	122.7
4c	-	220.1
5a	-	139.7
5b	-	146.9
5c	7.27	124.2
5d	7.38	127.7
<i>i</i> -Pr(CH)	2.82	29.4
<i>i</i> -Pr(CH <sub>3</sub> )	1.20 / 1.15	23.9 / 25.0

Figure 12. DPB...2iPr with assignment of  $^1\text{H}$  and  $^{13}\text{C}$  resonances.

*DPPD···2IPr*

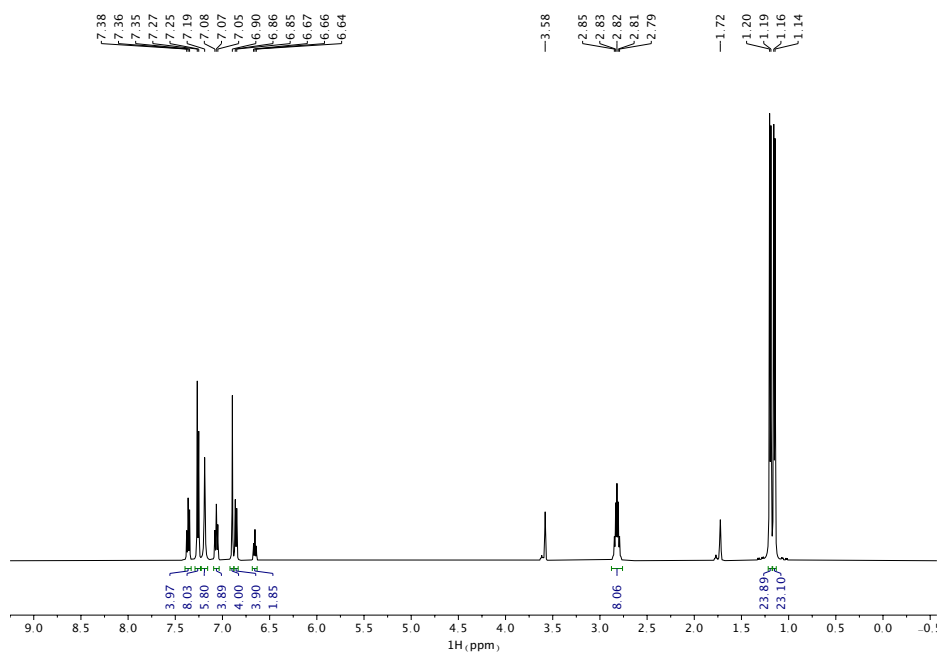


Figure 13.  $^1\text{H}$  NMR spectrum of **DPPD···2IPr** (50 mM,  $\text{THF}-d_8$ , 126 MHz, 298 K)

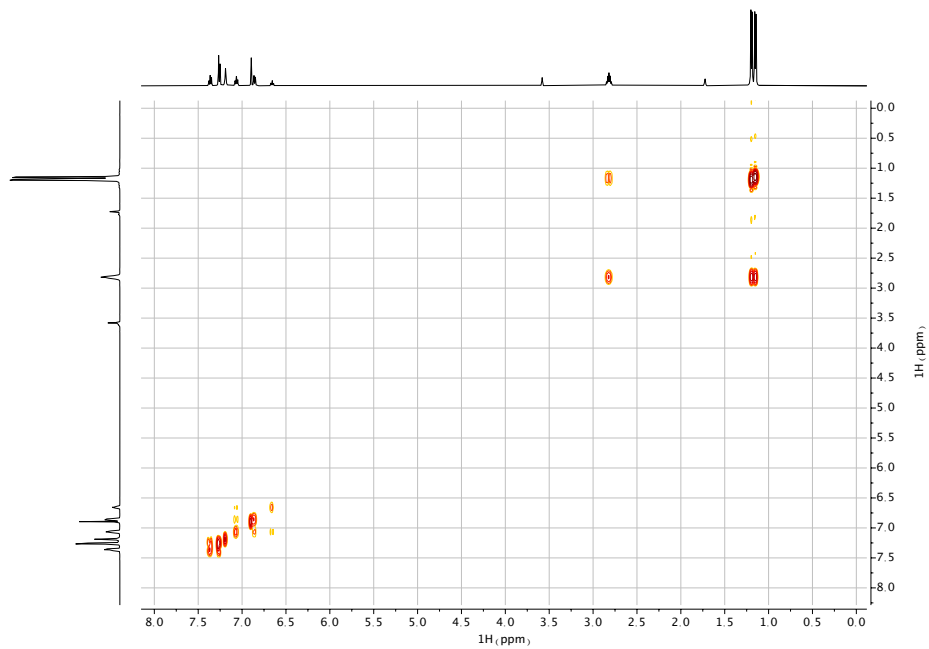


Figure 14.  $^1\text{H}$ - $^1\text{H}$  COSY spectrum of **DPPD···2IPr** (50 mM,  $\text{THF}-d_8$ , 500 MHz, 298 K)

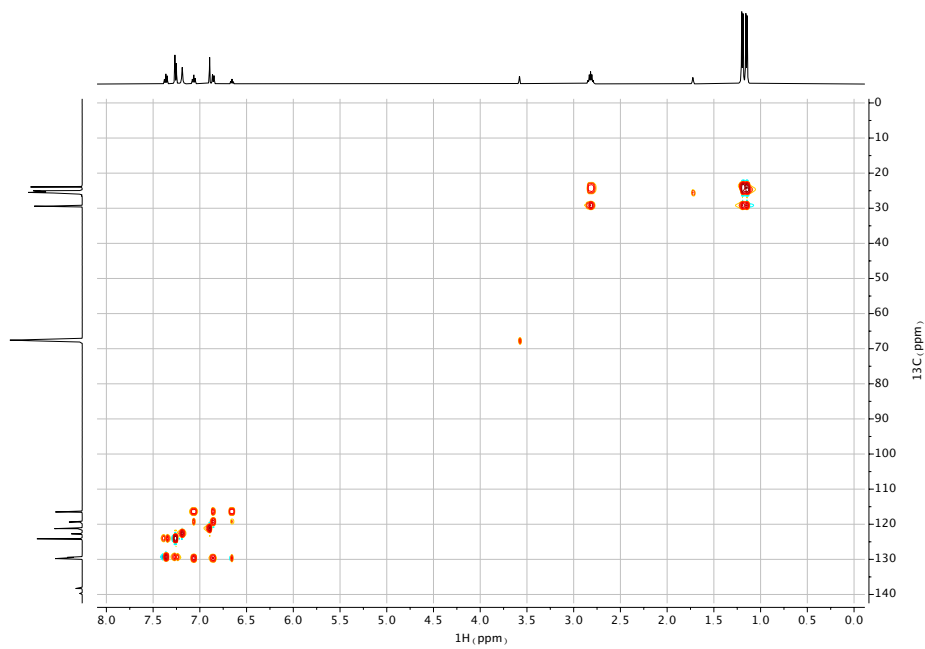


Figure 15.  $^1\text{H}$ - $^{13}\text{C}$  HSQC-TOCSY spectrum of **DPPD···2IPr** (50 mM,  $\text{THF}-d_8$ , 500 MHz, 298 K)

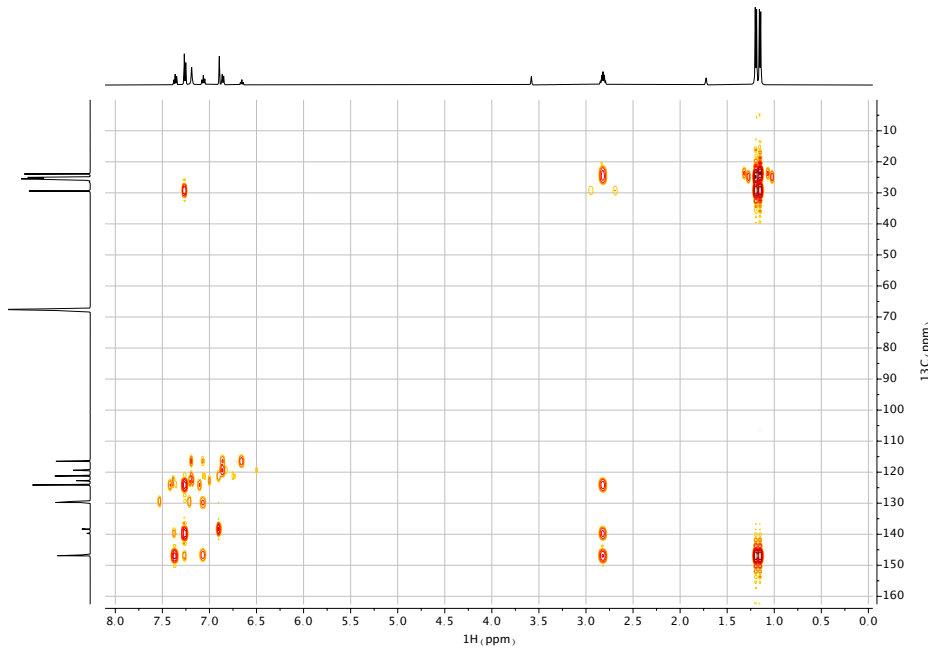


Figure 16.  $^1\text{H}$ - $^{13}\text{C}$  HMBC spectrum of **DPPD···2IPr** (50 mM,  $\text{THF}-d_8$ , 500 MHz, 298 K)

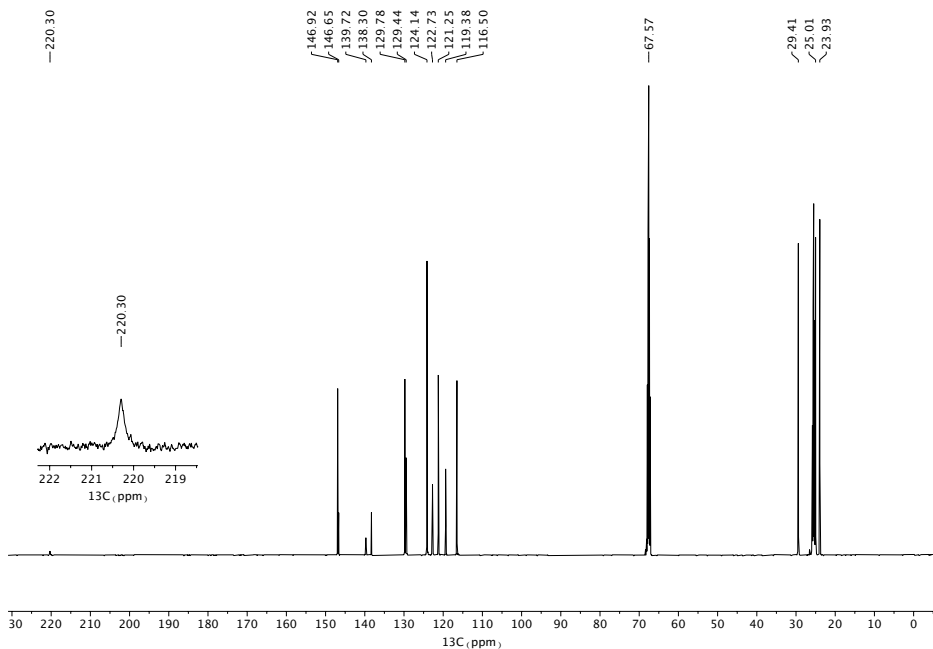
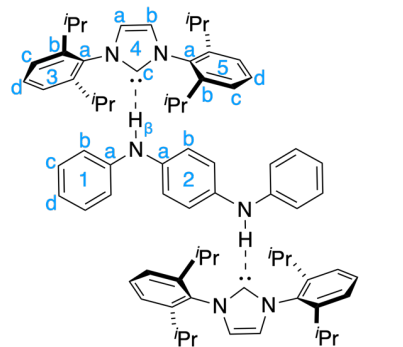


Figure 17.  $^{13}\text{C}\{^1\text{H}\}$  NMR spectrum of DPPD···2IPr (50 mM, THF- $d_8$ , 126 MHz, 298 K)



Assignment	$^1\text{H} \delta$	$^{13}\text{C} \delta$
1a	-	146.7
1b	6.86	116.5
1c	7.07	129.8
1d	6.66	119.4
2a	-	138.3
2b	6.9	121.3
$\text{H}_\beta$	7.19	-
3a	-	139.7
3b	-	146.9
3c	7.26	124.1
3d	7.36	129.4
4a	7.19	122.7
4b	7.19	122.7
4c	-	220.3
5a	-	139.7
5b	-	146.9
5c	7.26	124.1
5d	7.36	129.4
<i>i</i> -Pr(CH)	2.82	29.4
<i>i</i> -Pr(CH <sub>3</sub> )	1.19 / 1.15	23.9 / 25.0

Figure 18. DPPD···2IPr with assignment of  $^1\text{H}$  and  $^{13}\text{C}$  resonances.

DPA···IPr

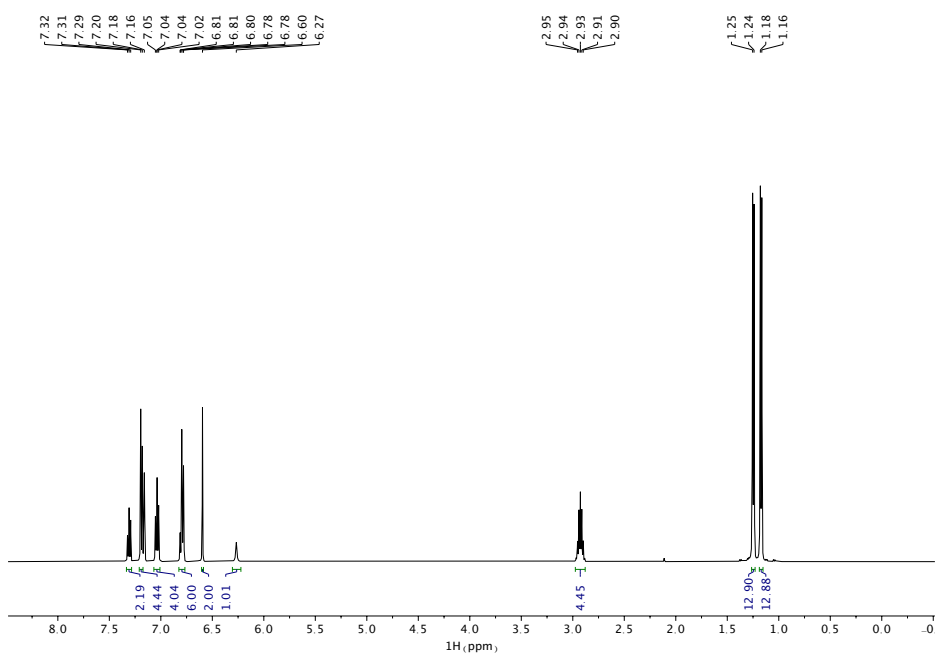


Figure 19.  $^1\text{H}$  NMR spectrum of DPA···IPr (75 mM,  $\text{C}_6\text{D}_6$ , 500 MHz, 298 K)

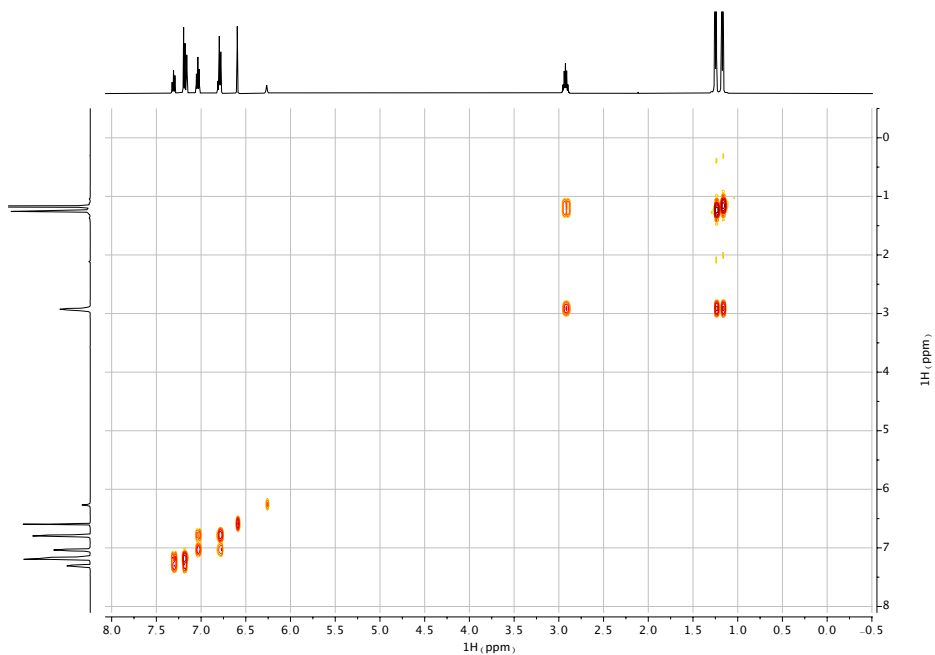


Figure 20.  $^1\text{H}$ - $^1\text{H}$  COSY spectrum of DPA···IPr (75 mM,  $\text{C}_6\text{D}_6$ , 500 MHz, 298 K)

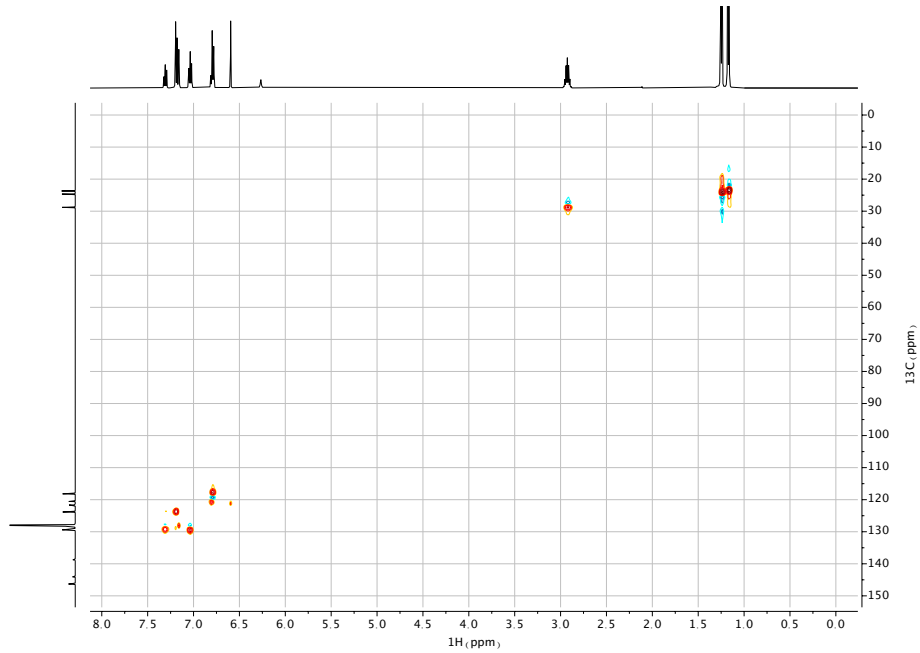


Figure 21.  $^1\text{H}$ - $^{13}\text{C}$  HSQC spectrum of DPA-IPr (75 mM,  $\text{C}_6\text{D}_6$ , 500 MHz, 298 K)

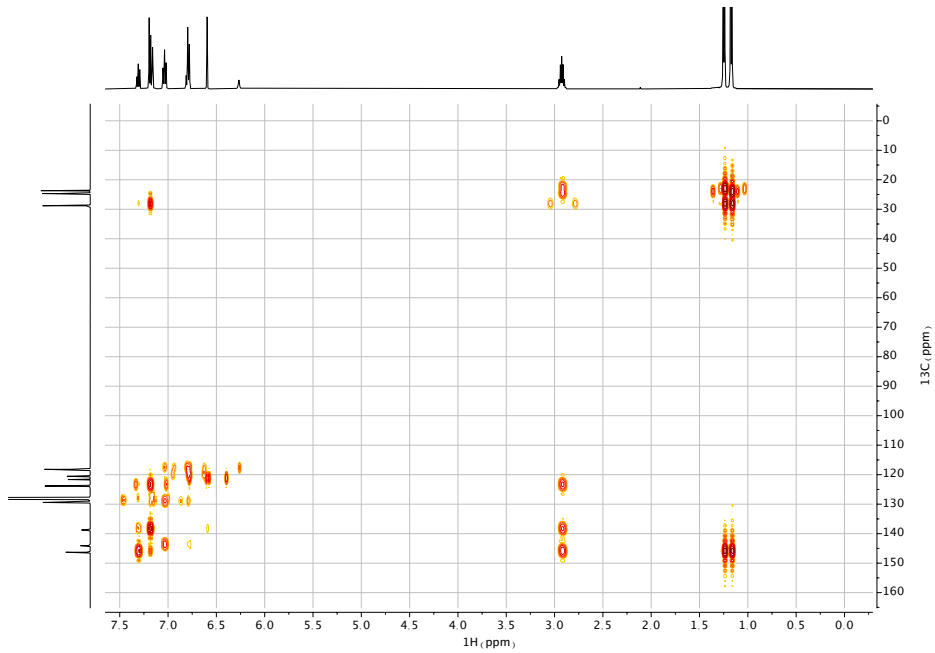


Figure 22.  $^1\text{H}$ - $^{13}\text{C}$  HMBC spectrum of DPA-IPr (75 mM,  $\text{C}_6\text{D}_6$ , 500 MHz, 298 K)

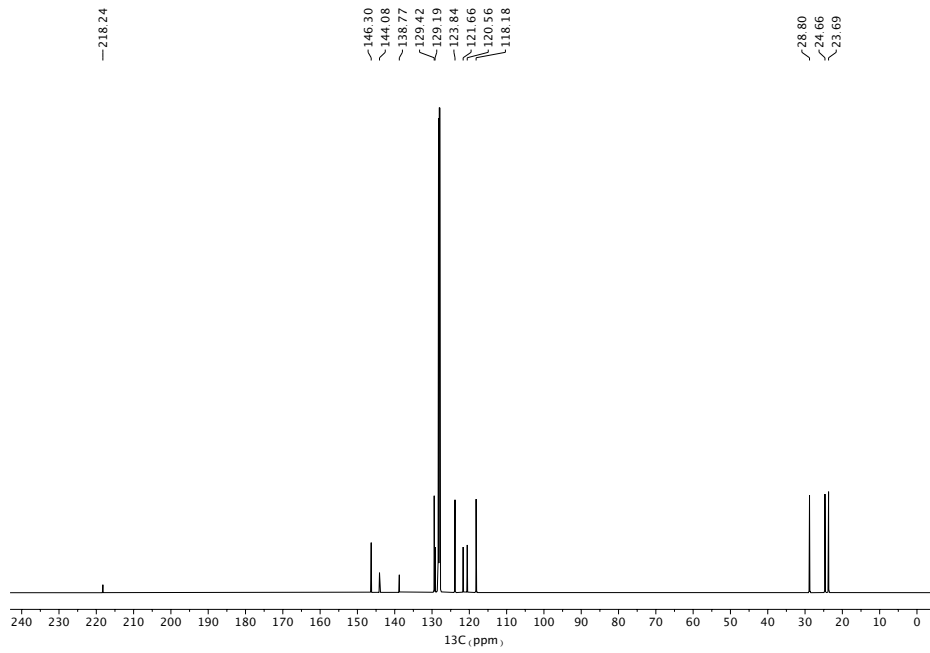
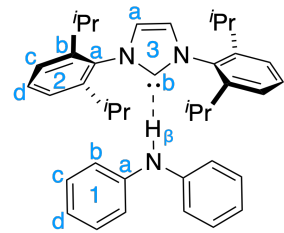


Figure 23.  $^{13}\text{C}\{^1\text{H}\}$  NMR spectrum of **DPA···IPr** (75 mM,  $\text{C}_6\text{D}_6$ , 126 MHz, 298 K)



Assignment	$^1\text{H}$ $\delta$	$^{13}\text{C}$ $\delta$
$\text{H}_\beta$	6.27	-
1a	-	144.1
1b	6.79	118.2
1c	7.04	129.4
1d	6.79	120.6
2a	-	138.8
2b	-	146.3
2c	7.19	123.8
2d	7.31	129.2
3a	6.6	121.7
3b	-	218.2
<i>i</i> -Pr(CH)	2.93	28.8
<i>i</i> -Pr(CH <sub>3</sub> )	1.25 / 1.17	24.7 / 23.7

Figure 24. **DPA···IPr** with assignment of  $^1\text{H}$  and  $^{13}\text{C}$  resonances.

CD

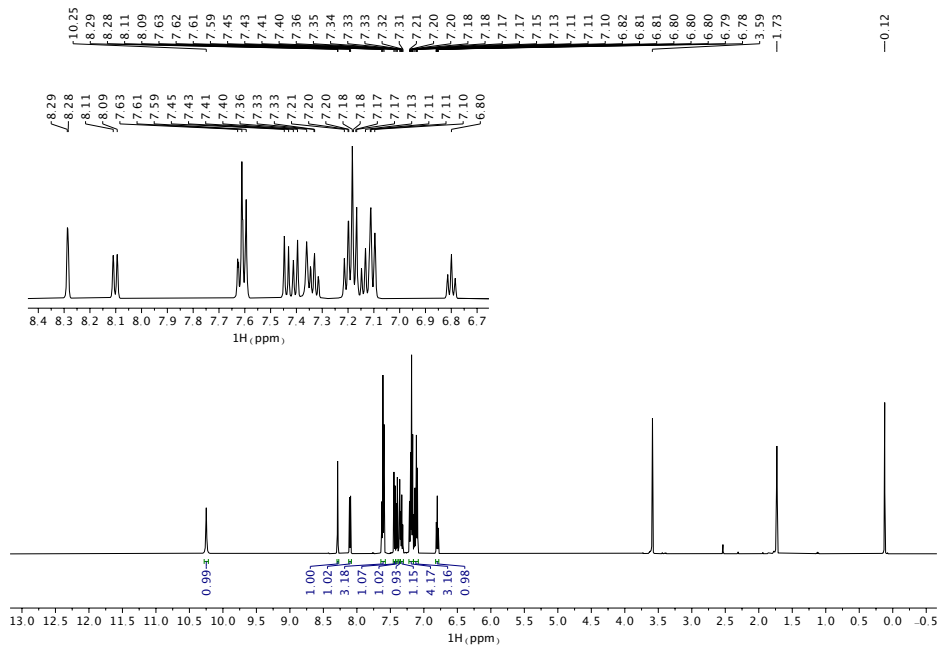


Figure 25.  $^1\text{H}$  NMR spectrum of **CD** (50 mM, THF- $d_8$ , 500 MHz, 298 K)

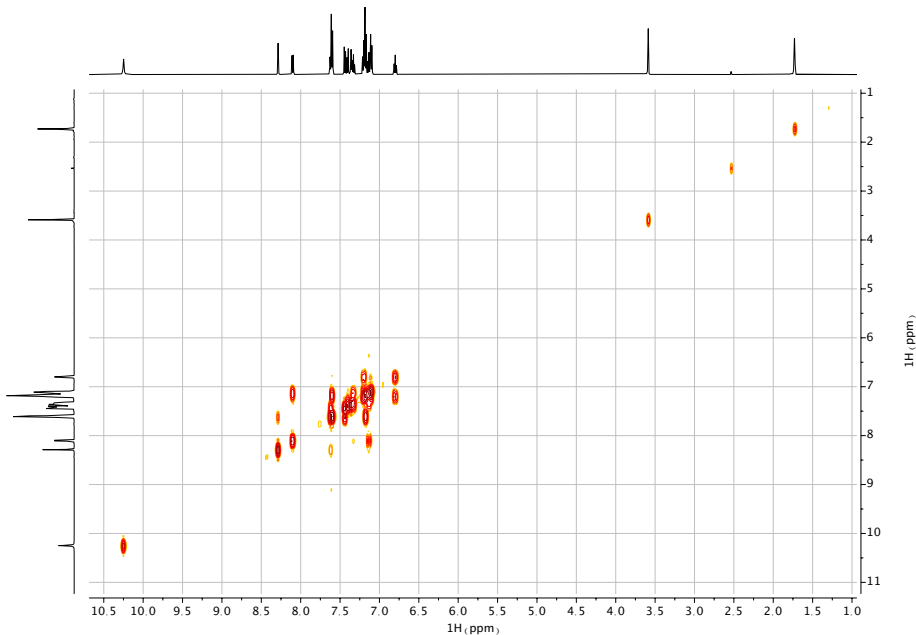


Figure 26.  $^1\text{H}$ - $^1\text{H}$  COSY spectrum of **CD** (50 mM, THF- $d_8$ , 500 MHz, 298 K)

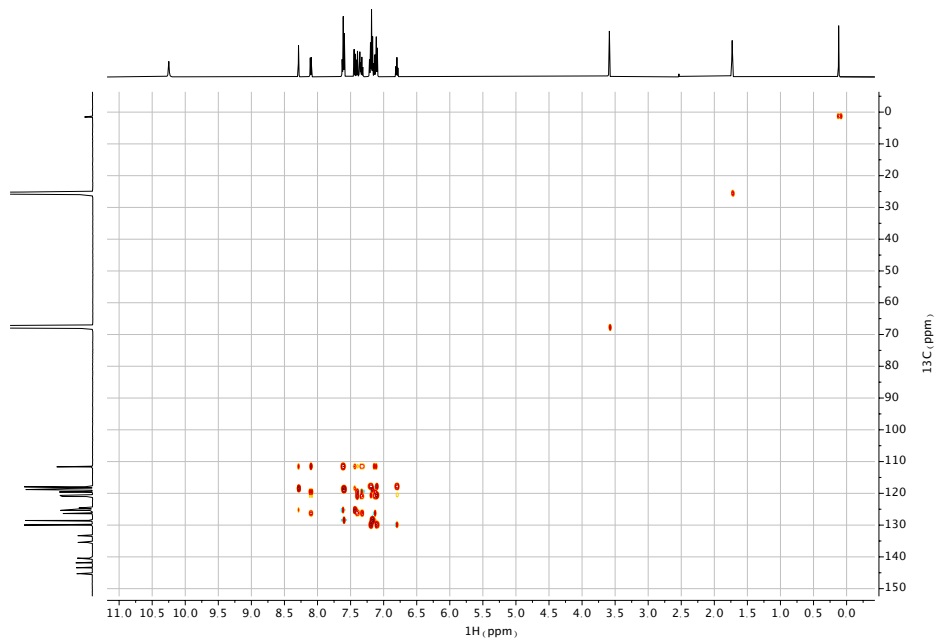


Figure 27.  $^1\text{H}$ - $^{13}\text{C}$  HQSC-TOCSY spectrum of **CD** (50 mM, THF- $d_8$ , 500 MHz, 298 K)

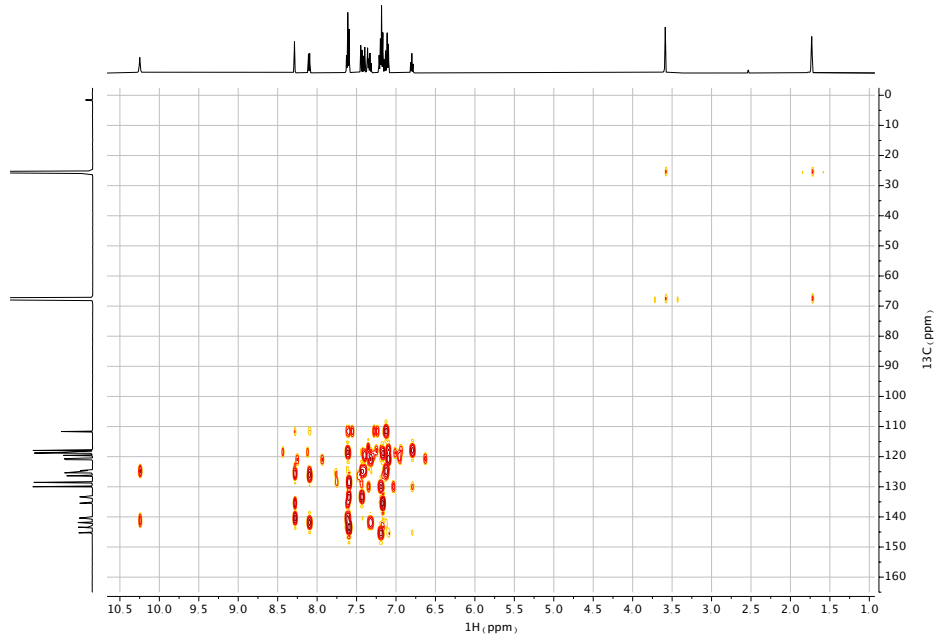


Figure 28.  $^1\text{H}$ - $^{13}\text{C}$  HMBC spectrum of **CD** (50 mM, THF- $d_8$ , 500 MHz, 298 K)

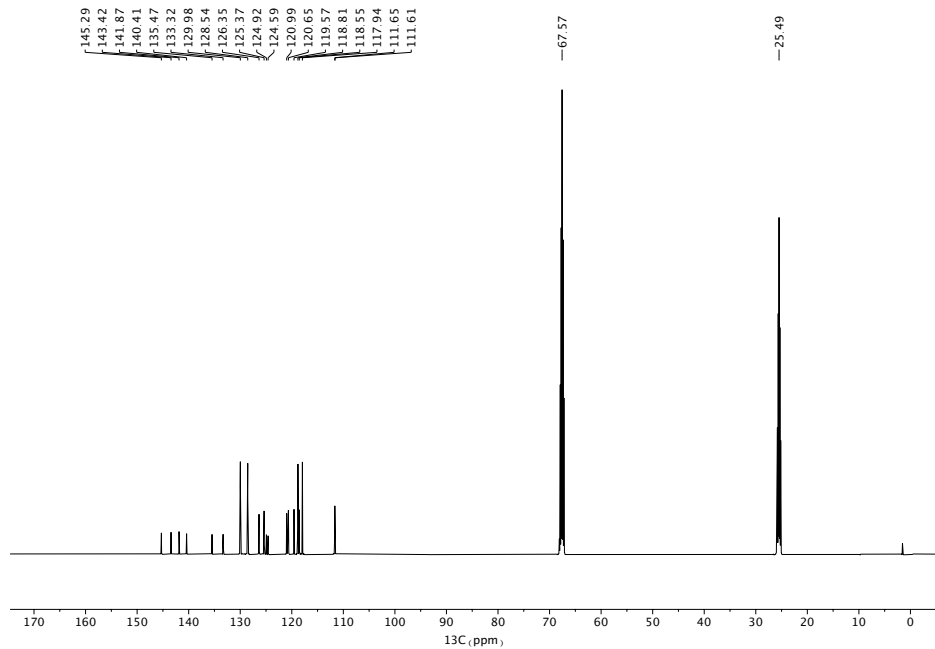
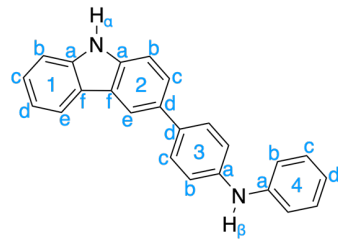


Figure 29.  $^{13}\text{C}\{\text{H}\}$  NMR spectrum of **CD** (50 mM, THF- $d_8$ , 126 MHz, 298 K)



Assignment	$^1\text{H} \delta$	$^{13}\text{C} \delta$
H <sub>a</sub>	10.25	-
1a	-	141.9
1b	7.40	111.6*
1c	7.33	126.4
1d	7.13	119.6
1e	8.10	121.0
1f	-	124.9
2a	-	140.4
2b	7.44	111.7*
2c	7.63	125.4
2d	-	133.3
2e	8.29	118.6
2f	-	124.6
H <sub>b</sub>	7.36	-
3a	-	143.4
3b	7.17	119.6
3c	7.60	128.5
3d	-	135.5
4a	-	145.3
4b	7.10	117.9
4c	7.19	130.0
4d	6.80	120.7

Figure 30. **CD** with assignment of  $^1\text{H}$  and  $^{13}\text{C}$  resonances,  $^{13}\text{C}$  signals labeled \* are indistinguishable.

CD ··· 2IPr

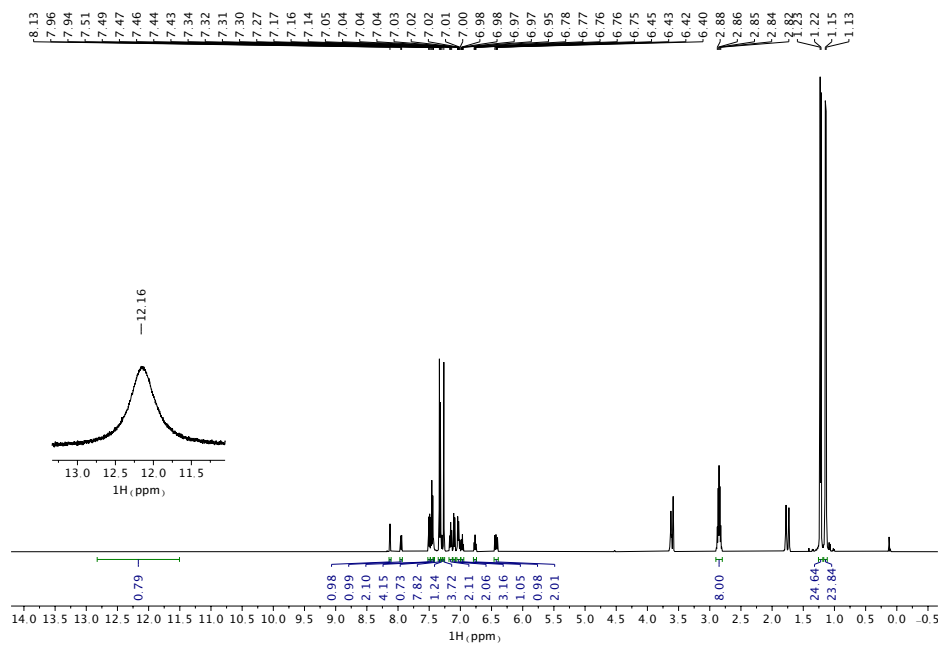


Figure 31.  $^1\text{H}$  NMR spectrum of **CD** $\cdots$ **2IPr** (50 mM, THF- $d_8$ , 500 MHz, 298 K)

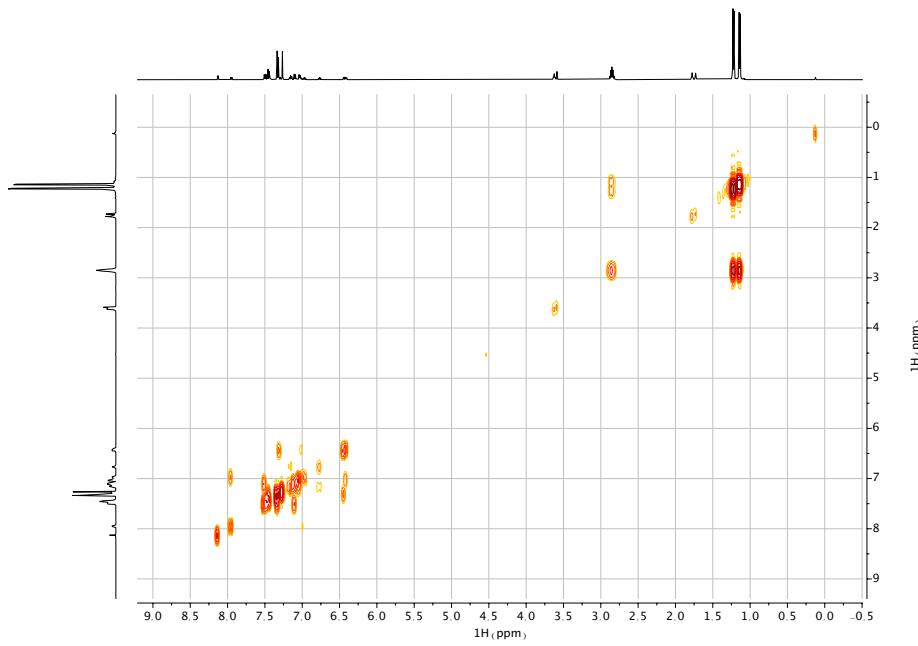


Figure 32.  $^1\text{H}$ - $^1\text{H}$  COSY spectrum of **CD** $\cdots$ **2IPr** (50 mM, THF- $d_8$ , 500 MHz, 298 K)

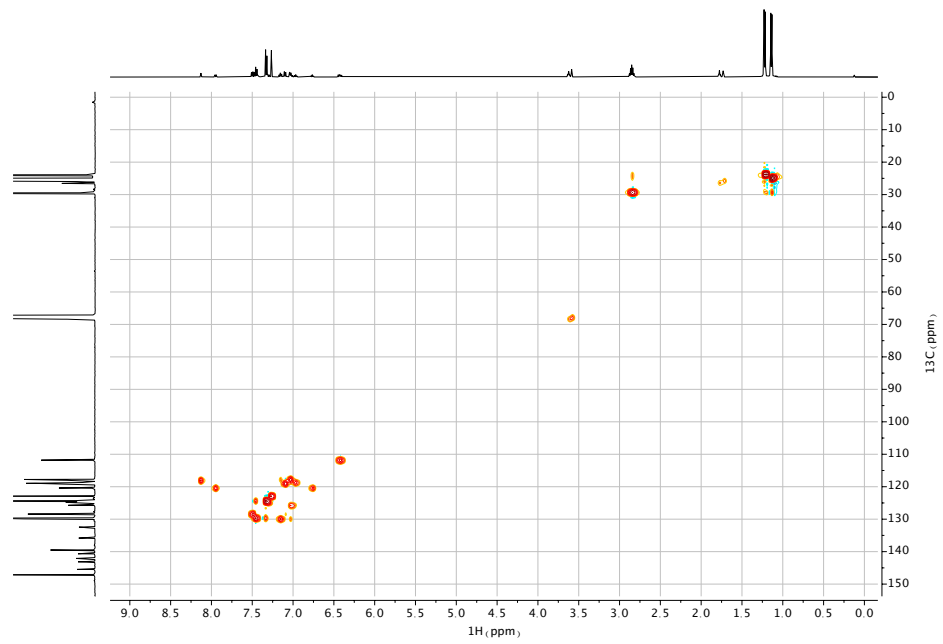


Figure 33. <sup>1</sup>H-<sup>13</sup>C HSQC spectrum of **CD···2IPr** (50 mM, THF-*d*<sub>8</sub>, 500 MHz, 298 K)

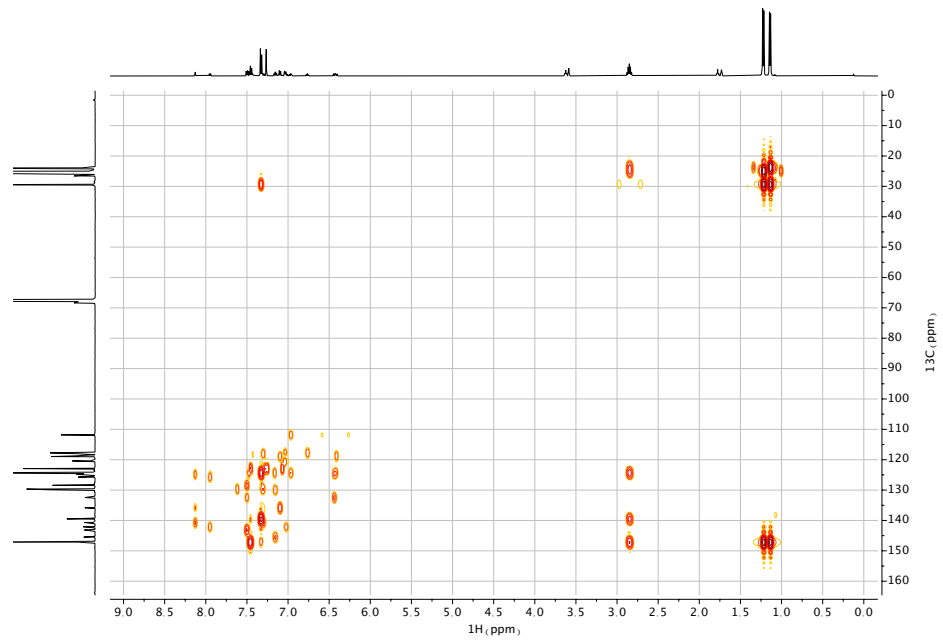


Figure 34. <sup>1</sup>H-<sup>13</sup>C HMBC spectrum of **CD···2IPr** (50 mM, THF-*d*<sub>8</sub>, 500 MHz, 298 K)

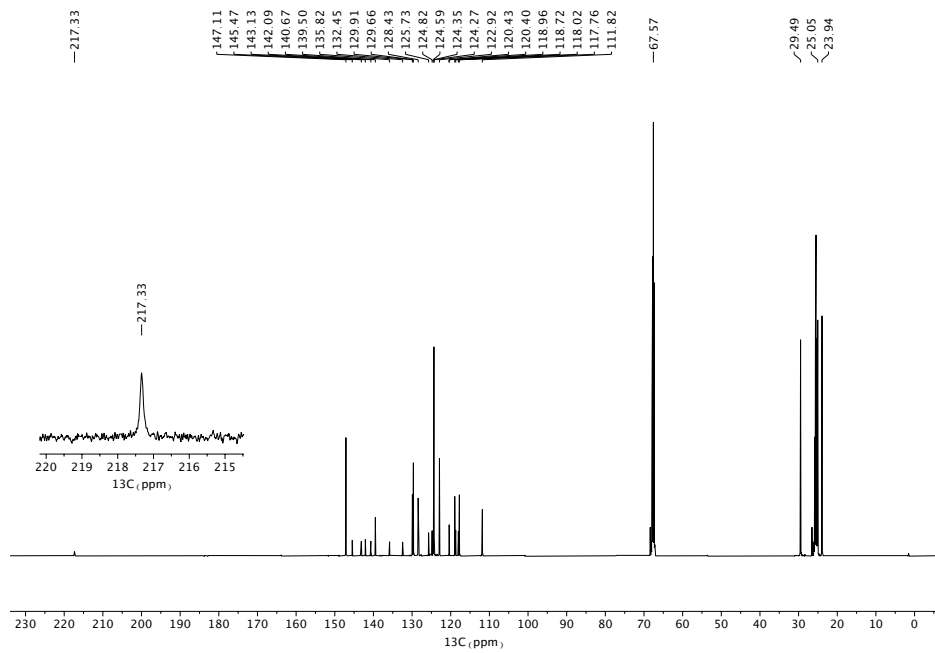
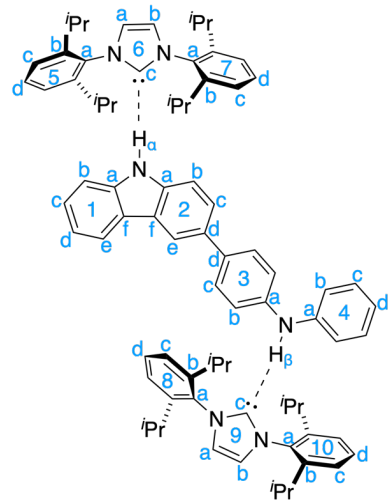


Figure 35.  $^{13}\text{C}\{\text{H}\}$  NMR spectrum of **CD···2IPr** (50 mM, THF- $d_8$ , 126 MHz, 298 K)



Assignment	$^1\text{H}$ δ	$^{13}\text{C}$ δ	Assignment	$^1\text{H}$ δ	$^{13}\text{C}$ δ
H <sub>α</sub>	12.16	-	5a	-	139.5
1a	-	142.1	5b	-	147.1
1b	6.41	111.8	5c	7.33	124.4
1c	7.02	125.7	5d	7.46	129.7
1d	6.97	118.7	6a	7.27	122.9
1e	7.95	120.4*	6b	7.27	122.9
1f	-	124.3	6c	-	217.3
2a	-	140.7	7a	-	139.5
2b	6.44	111.8	7b	-	147.1
2c	7.3	124.8	7c	7.33	124.4
2d	-	132.5	7d	7.46	129.7
2e	8.13	118.0	i-Pr(CH)	2.85	29.5
2f	-	124.6	i-Pr(CH <sub>3</sub> )	1.14 / 1.22	25.0 / 23.9
H <sub>β</sub>	7.43	-	8a	-	139.5
			8b	-	147.1
			8c	7.33	124.4
3a	-	143.1	8d	7.46	129.7
3b	7.1	119.0	9a	7.27	122.9
3c	7.5	128.4	9b	7.27	122.9
3d	-	135.8	9c	-	217.3
4a	-	145.5	10a	-	139.5
4b	7.02	117.8	10b	-	147.1
4c	7.15	129.9	10c	7.33	124.4
4d	6.76	120.4*	10d	7.46	129.7
			i-Pr(CH)	2.85	29.5
			i-Pr(CH <sub>3</sub> )	1.14 / 1.22	25.0 / 23.9

Figure 36. **CD···2iPr** with assignment of  $^1\text{H}$  and  $^{13}\text{C}$  resonances,  $^{13}\text{C}$  signals labeled \* are indistinguishable.

**CD···IPr**

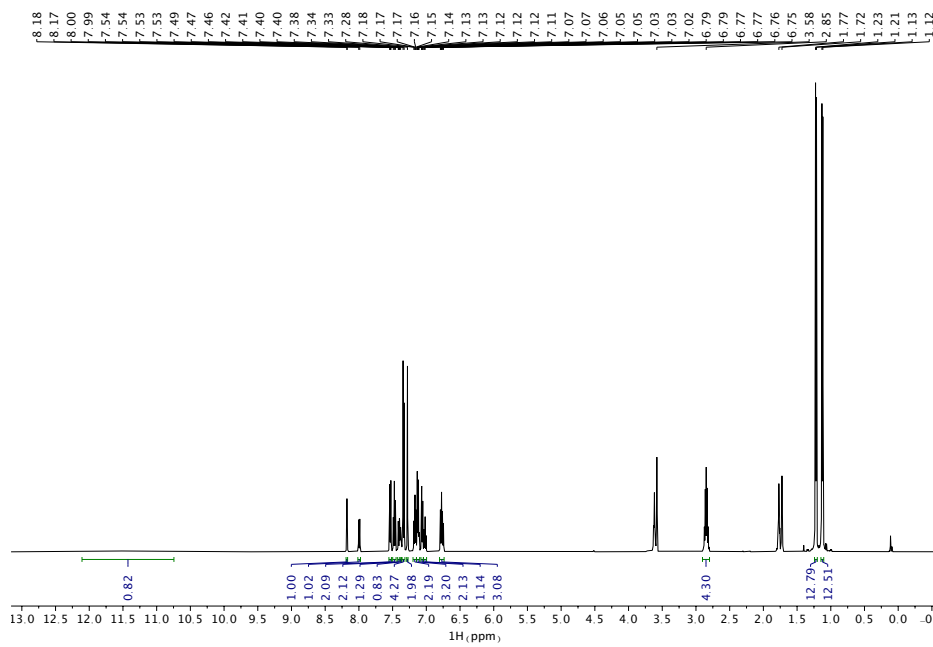


Figure 37. <sup>1</sup>H NMR spectrum of **CD···IPr** (50 mM, THF-*d*<sub>8</sub>, 500 MHz, 298 K)

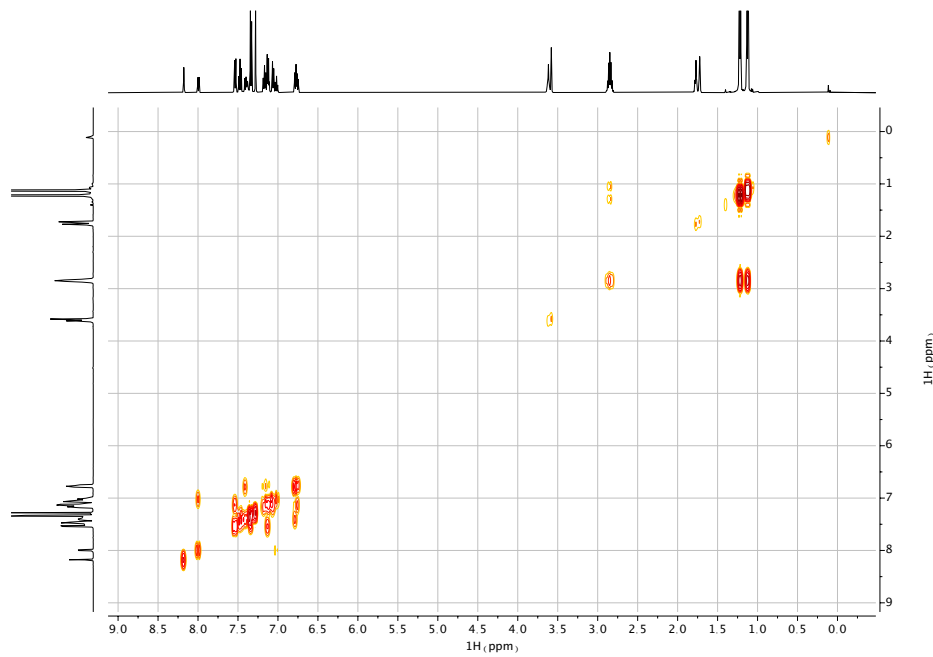


Figure 38. <sup>1</sup>H-<sup>1</sup>H COSY spectrum of **CD···IPr** (50 mM, THF-*d*<sub>8</sub>, 500 MHz, 298 K)

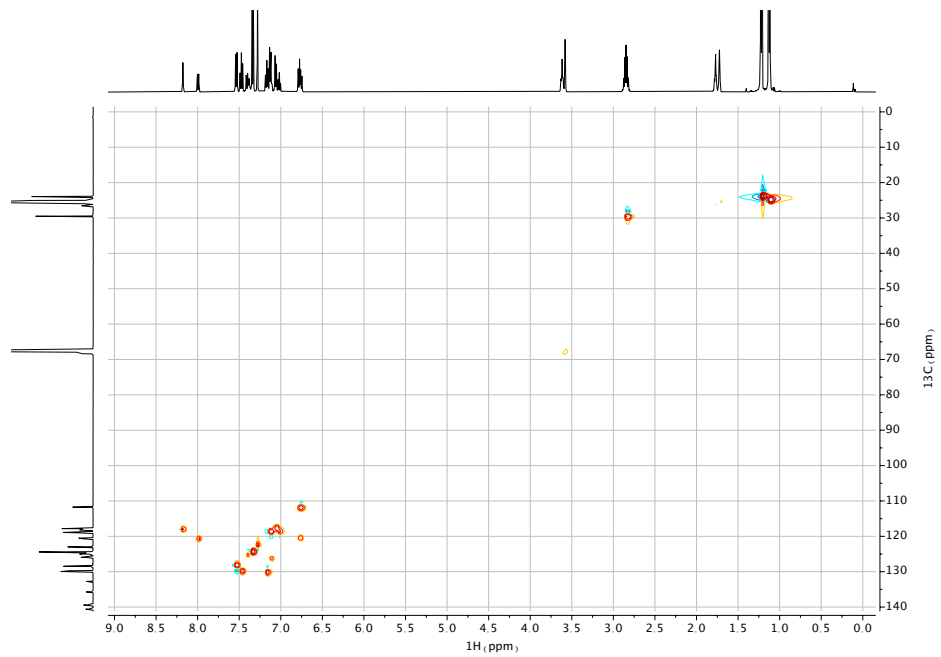


Figure 39.  $^1\text{H}$ - $^{13}\text{C}$  HSQC spectrum of **CD…IPr** (50 mM, THF- $d_8$ , 500 MHz, 298 K)

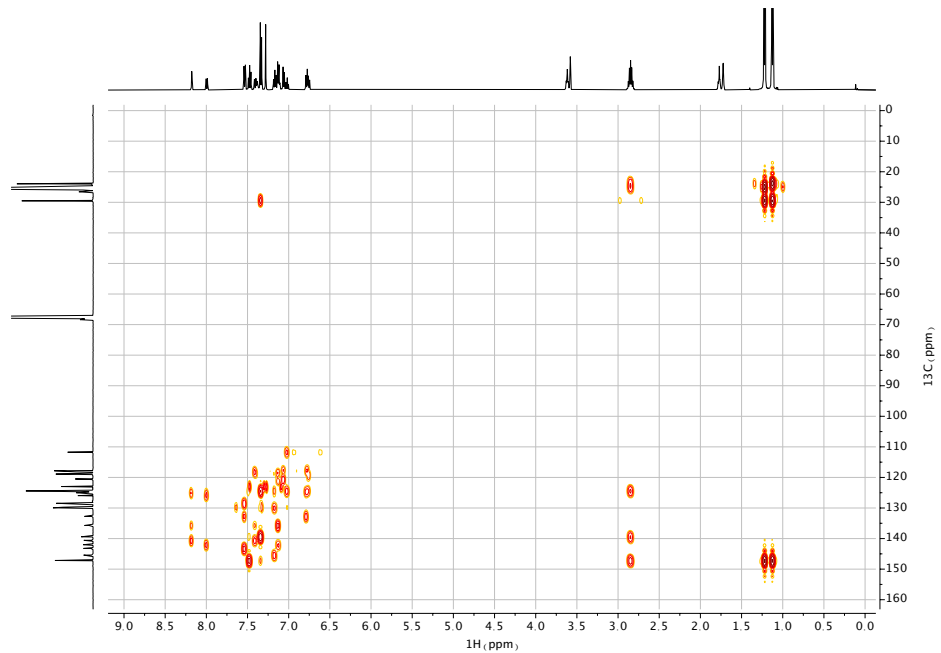


Figure 40.  $^1\text{H}$ - $^{13}\text{C}$  HMBC spectrum of **CD…IPr** (50 mM, THF- $d_8$ , 500 MHz, 298 K)

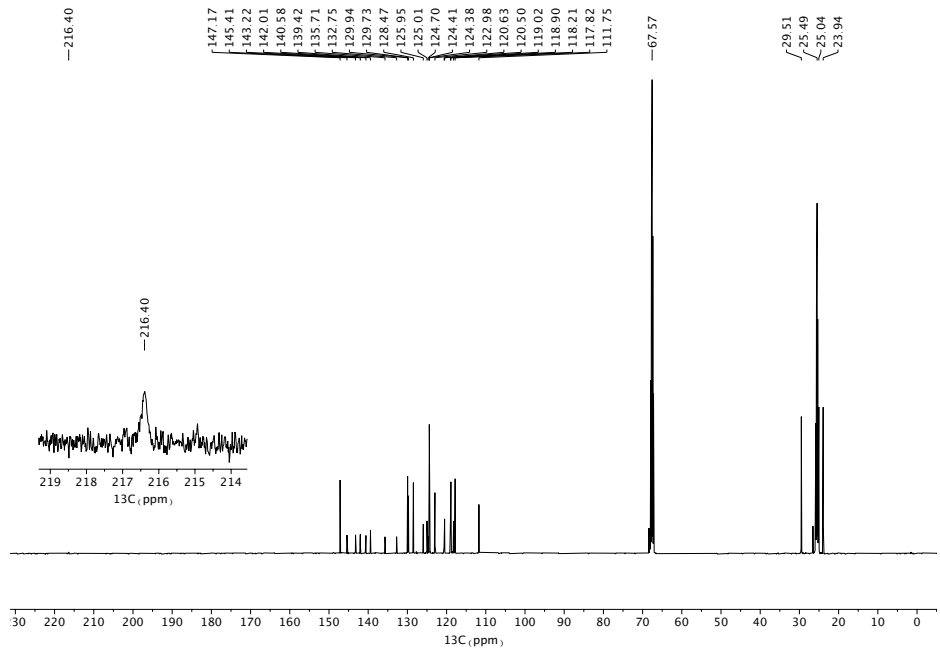
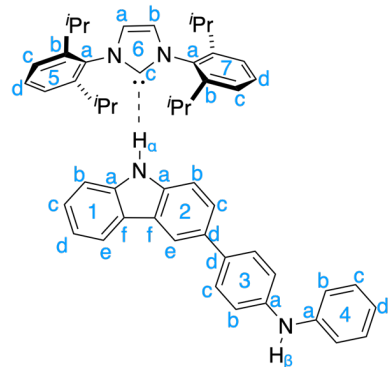


Figure 41.  $^{13}\text{C}\{^1\text{H}\}$  NMR spectrum of **CD···IPr** (50 mM,  $\text{THF-}d_8$ , 126 MHz, 298 K)



Assignment	$^1\text{H } \delta$	$^{13}\text{C } \delta$
$\text{H}_\alpha$	11.47	-
1a	-	142.0
1b	6.78	111.8
1c	7.11	126.0
1d	7.02	119.0
1e	7.99	120.6
1f	-	124.7
2a	-	140.6
2b	6.78	111.8
2c	7.41	125.0
2d	-	132.8
2e	8.18	118.2
2f	-	124.4
$\text{H}_\beta$	7.38	-
3a	-	143.2
3b	7.13	118.9
3c	7.53	128.5
3d	-	135.7
4a	-	145.4
4b	7.06	117.8
4c	7.17	129.9
4d	6.75	120.5
5a	-	139.4
5b	-	147.2
5c	7.34	124.4
5d	7.47	129.7
6a	7.28	123.0
6b	7.28	123.0
6c	-	216.4
7a	-	139.4
7b	-	147.2
7c	7.34	124.4
7d	7.47	129.7
$i\text{-Pr}(\text{CH})$	2.85	29.5
$i\text{-Pr}(\text{CH}_3)$	1.22 / 1.12	23.9 / 25.0

Figure 42. **CD···IPr** with assignment of  $^1\text{H}$  and  $^{13}\text{C}$  resonances.

### 3) $^1\text{H}$ NMR Comparison of Parent Amines to Adducts

Comparison of parent amine  $^1\text{H}$  resonances to adducts. All spectra were acquired in THF- $d_8$  at a concentration of 50 mM.  $\Delta\delta$  is calculated by subtracting the parent chemical shift from the adduct. Positive  $\Delta\delta$  indicate a downfield shift, while negative  $\Delta\delta$  indicate an upfield shift.

**BC···2*iPr***

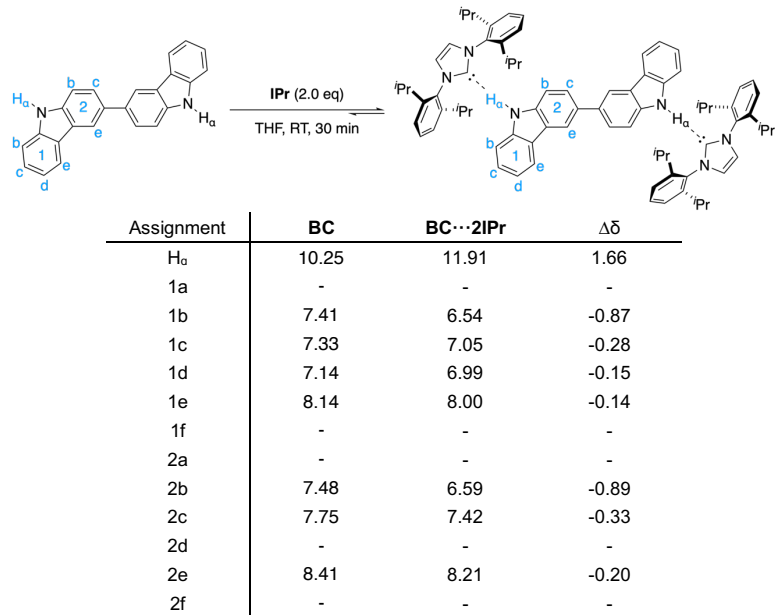


Figure 43.  $^1\text{H}$  chemical shift comparison of **BC···2*iPr*** adduct to parent **BC**.

**DPB···2*iPr***

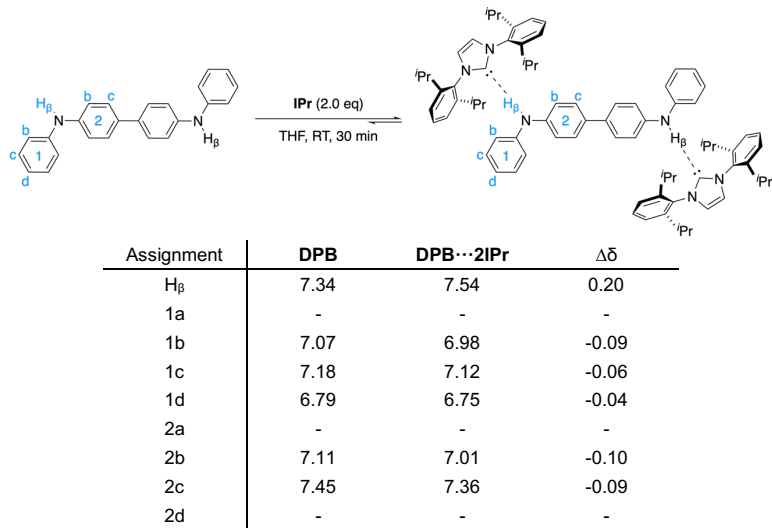


Figure 44.  $^1\text{H}$  chemical shift comparison of **DPB···2*iPr*** adduct to parent **DPB**.

*DPPD···2IPr*

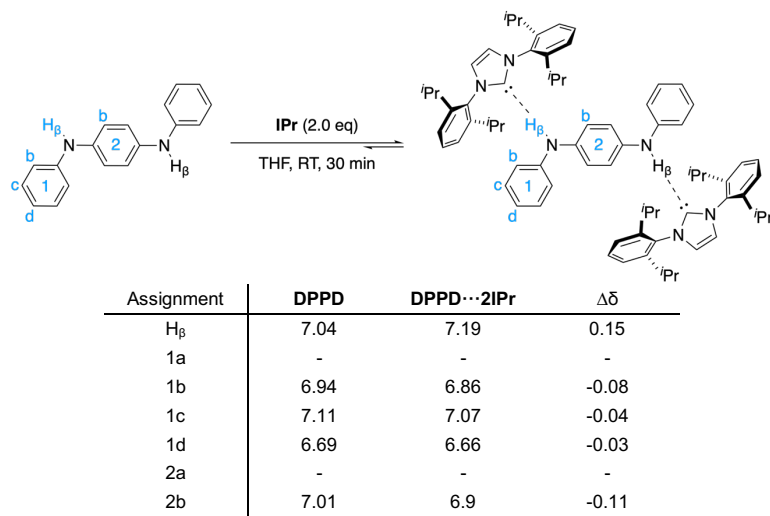


Figure 45.  $^1\text{H}$  chemical shift comparison of **DPPD···2IPr** adduct to parent **DPPD**.

*CD···2IPr*

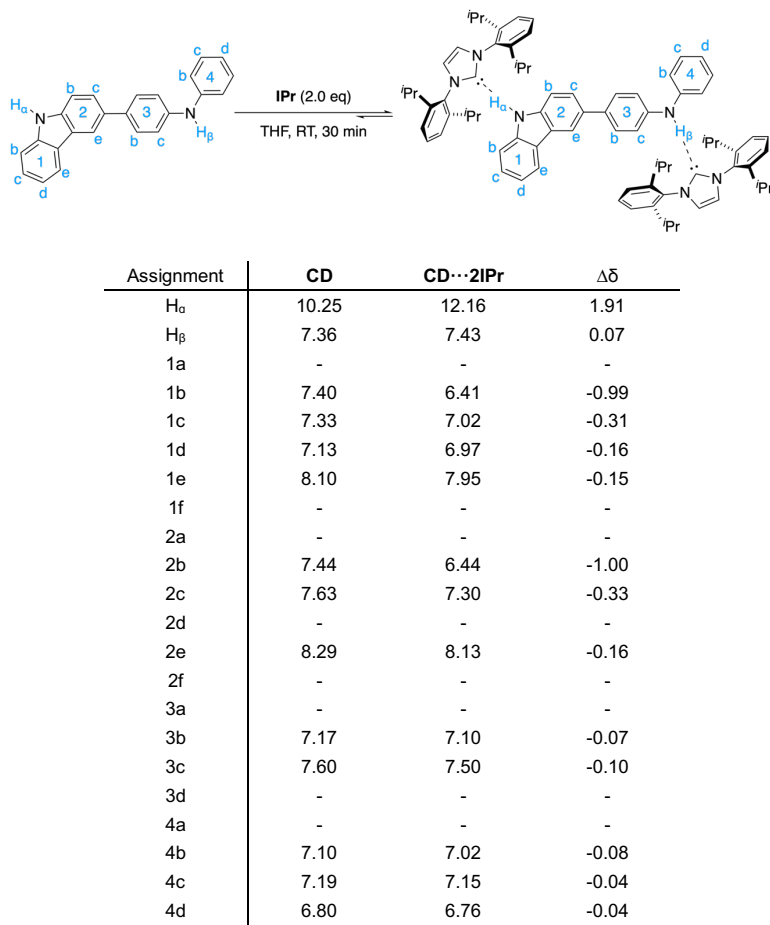
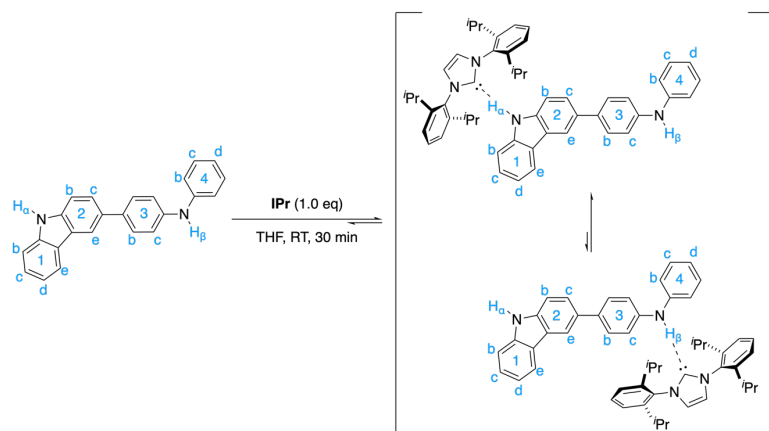


Figure 46.  $^1\text{H}$  chemical shift comparison of **CD···2IPr** adduct to parent **CD**.

**CD···IPr**



Assignment	CD	CD···IPr	$\Delta\delta$
H <sub>α</sub>	10.25	11.47	1.22
H <sub>β</sub>	7.36	7.38	0.02
1a	-	-	-
1b	7.40	6.78	-0.62
1c	7.33	7.11	-0.22
1d	7.13	7.02	-0.11
1e	8.10	7.99	-0.11
1f	-	-	-
2a	-	-	-
2b	7.44	6.78	-0.66
2c	7.63	7.41	-0.22
2d	-	-	-
2e	8.29	8.18	-0.11
2f	-	-	-
3a	-	-	-
3b	7.17	7.13	-0.04
3c	7.60	7.53	-0.07
3d	-	-	-
4a	-	-	-
4b	7.10	7.06	-0.04
4c	7.19	7.17	-0.02
4d	6.80	6.75	-0.05

Figure 47. <sup>1</sup>H chemical shift comparison of **CD···IPr** adduct to parent **CD**.

#### 4) Evaluation of DPA···IPr Hydrogen Bond Strength

*Concentration dependent  $^1\text{H}$  NMR analysis*

A series of **DPA···IPr** solutions in  $\text{C}_6\text{D}_6$  were probed via  $^1\text{H}$  NMR spectroscopy to measure the strength of the N–H···C $\leq$  interaction.<sup>5,6</sup> Over the concentration range probed (75–1 mM, actual concentrations see Table S1) only the NH resonance shift,  $\text{H}_\beta$ , was significant enough to fit. Fitting the data in the same manner as done previously<sup>5</sup> gives a  $K_d$  of  $0.85 \pm 1.05 \text{ M}^{-1}$ , which yields a  $\Delta G \approx -0.10 \text{ kcal mol}^{-1}$  for the strength of this association. These data sets could also be fit using a 1:1 association model in Bindfit,<sup>7</sup> which confirms our finding (**DPA···IPr** NH fitting from Bindfit:  $K_d$  of  $0.85 \pm 0.02 \text{ M}^{-1}$ ,  $\Delta G \approx -0.10 \text{ kcal mol}^{-1}$ ).

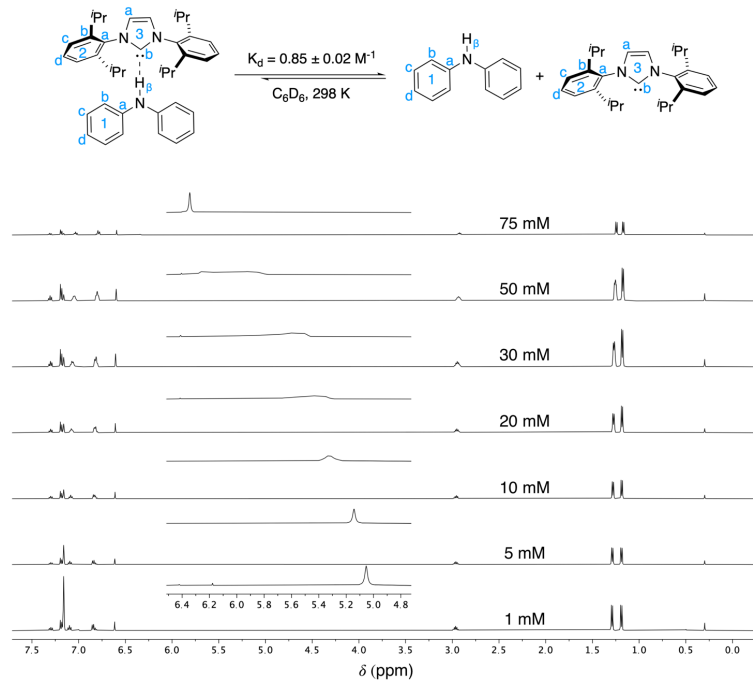


Figure 48.  $^1\text{H}$  NMR spectra of **DPA···IPr** (75–1 mM,  $\text{C}_6\text{D}_6$ , 500 MHz, 298K). Inset of  $\text{H}_\beta$  exchanging over this concentration range.

Conc. (mM)	$\text{H}_\beta$	1b	1c	1d	2c	2d	$\text{Pr}(\text{CH})$	$\text{Pr}(\text{CH}_3)$	$\text{Pr}(\text{CH}_3)'$	3a
75.2	6.34	6.79	7.03	6.80	7.19	7.31	2.92	1.24	1.17	6.59
50.2	6.07	6.80	7.05	6.80	7.19	7.31	2.94	1.26	1.18	6.60
30.1	5.56	6.82	7.07	6.82	7.19	7.31	2.95	1.27	1.18	6.60
20.1	5.42	6.83	7.08	6.83	7.19	7.30	2.95	1.28	1.18	6.61
10.0	5.32	6.83	7.09	6.82	7.19	7.30	2.96	1.28	1.18	6.61
5.0	5.13	6.84	7.09	6.82	7.19	7.30	2.96	1.29	1.18	6.61
1.0	5.05	6.85	7.10	6.82	7.19	7.30	2.96	1.29	1.19	6.61
$\Delta\delta =$	-1.29	0.06	0.07	0.02	0.00	-0.01	0.04	0.05	0.02	0.02

Table 1.  $^1\text{H}$  chemical shifts for **DPB···2IPr** over 75–1 mM ( $\text{C}_6\text{D}_6$ , 500 MHz, 298K),  $\text{H}_\beta$  used in analysis.

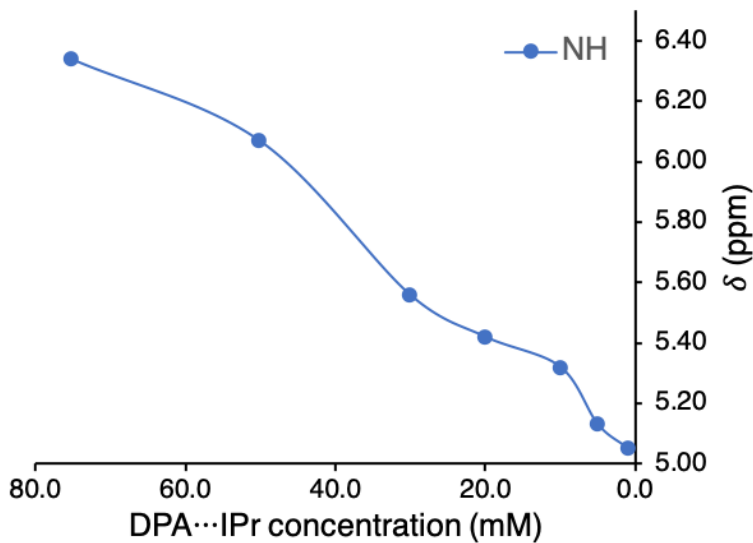


Figure 49. Plot of  $\delta$  (ppm) vs DPA···IPr (mM).

#### Amine Exchange

To demonstrate the labile nature of the DPA···IPr adduct an exchange experiment wherein 1.0 equivalent of Cbz was added to a premade solution of DPA···IPr in THF was performed. After the removal of solvent reaction mixture was probed via  $^1\text{H}$  NMR revealing nearly complete conversion to Cbz···IPr and release of DPA. The blacked dotted lines in Figure 50 show the similarities to Cbz···IPr, while the orange lines track the differences in DPA-based signals. All spectra of adducts were prepared at 75 mM in  $\text{C}_6\text{D}_6$ .

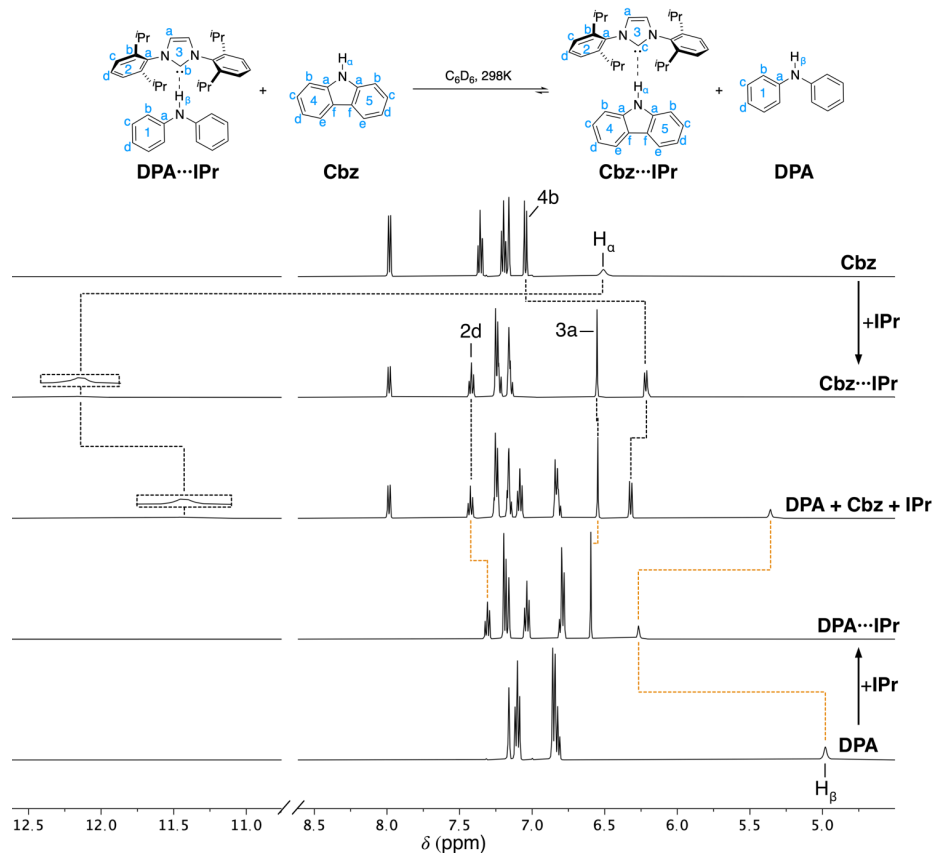


Figure 50. Partial  $^1\text{H}$  NMR spectra (500 MHz,  $\text{C}_6\text{D}_6$ ) of Cbz···IPr, equilibrium mixture of DPA, Cbz, and IPr, and DPA···IPr.

## 5) Crystallographic Analysis

Data for **BC···2IPr**, **DPPD···2IPr**, and **CD** were collected using a Bruker Micro-State diffractometer using a rotating-anode Cu-radiation source with APEX II detector and micro-focus optics. The resulting structures followed routine procedures accompanied with software packages for data collection from Bruker XRD and refinement using the OLEX2 system.

### **BC···2IPr**

A single crystal of **BC···2IPr** was obtained through vapor diffusion of hexanes into a saturated solution of **BC···2IPr** in THF. In the crystal structure the bicarbazole moiety sits at an inversion center, thus consisting of two distinct **BC···2IPr** structures with slight variability. Each structure is given below (identified as **BC···2IPr-A** and **BC···2IPr-B**) with the following average bond lengths ( $\text{\AA}$ ) and angles ( $^\circ$ ): H1···C13, 2.10; N1···C13, 2.96; N2–C13–N3, 102.2; N1–H1···C13, 168; N2–N3–C12–C1, 13.5. **BC:2IPr** was obtained as a co-crystal with THF (shown in each figure). Hydrogens not participating in hydrogen bonding have been removed for clarity. CCDC number: 2011390

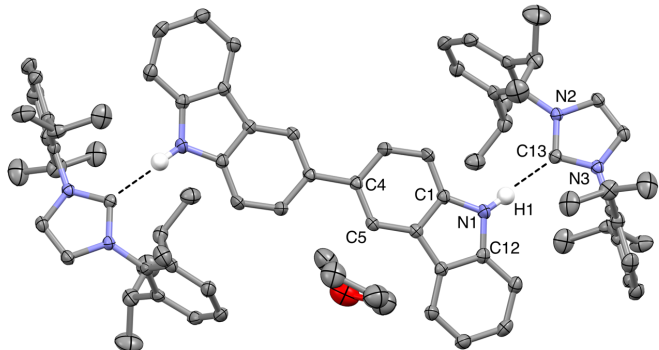


Figure 51. ORTEP diagram of **BC···2IPr-A** adduct (ellipsoids drawn at 50% probability). Non-hydrogen bonding hydrogens have been omitted for clarity. Select bond lengths ( $\text{\AA}$ ) and angles ( $^\circ$ ): H1···C13, 2.09(2); N1···C13, 2.980(2); N2–C13–N3, 102.4(1); N1–H1···C13, 177(2); N2–N3–C12–C1, 15.25(7)

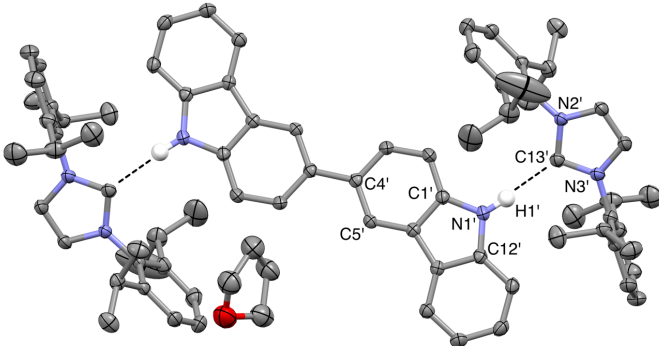


Figure 52. ORTEP diagram of **BC···2IPr-B** adduct (ellipsoids drawn at 50% probability). Non-hydrogen bonding hydrogens have been omitted for clarity. Select bond lengths ( $\text{\AA}$ ) and angles ( $^\circ$ ): H1'···C13', 2.112; N1'···C13', 2.951(2); N2'–C13'–N3', 102.0(1); N1'–H1'···C13', 159.01; N2'–N3'–C12'–C1', -11.70(7)

	<b>BC···2IPr Adduct</b>
Empirical Formula	<chem>C62H96N6O</chem>
Formula Weight	1181.64
Temperature	100.0 K
Wavelength	1.54178 Å
Crystal System	Triclinic
Space Group	P-1
a	12.7938(2) Å
b	14.3012(2) Å
c	19.4614(2) Å
$\alpha$	78.6270(10) °
$\beta$	72.4790(10) °
$\gamma$	74.7170(10) °
Volume	3502.44(8) Å <sup>3</sup>
Z	2
Density (calculated)	1.120 Mg/m <sup>3</sup>
Absorption Coefficient	0.501 mm <sup>-1</sup>
F (000)	1276
Crystal Size	0.29 x 0.27 x 0.25 mm <sup>3</sup>
Theta range for data collection	2.400 to 68.344 °
Index Ranges	-16<=h<=16, -17<=k<=17, -23<=l<=23
Reflections Collected	56480
Independent Reflections	12561 [R(int) = 0.0294]
Completeness to Theta = 67.679 °	97.7 %
Absorption Correction	Semi-empirical from equivalents
Max. and Min. Transmission	0.7531 and 0.6751
Refinement Method	Full-matrix least-squares on F <sup>2</sup>
Data / Restraints / Parameters	12561 / 0 / 822
Goodness-of-fit on F <sup>2</sup>	1.045
Final R Indices [ >2sigma( )]	R1 = 0.0453, wR2 = 0.1199
R indices (all data)	R1 = 0.0505, wR2 = 0.1249
Largest Diff. Peak and Hole	0.536 and -0.413 e.Å <sup>-3</sup>

**DPPD···2IPr**

A single crystal of **DPPD···2IPr** was obtained through storage at -35 °C for several days in a hexanes:THF 3:2 mixture. The reddish-brown crystals obtained were suitable for X-ray diffraction. CCDC number: 2011391

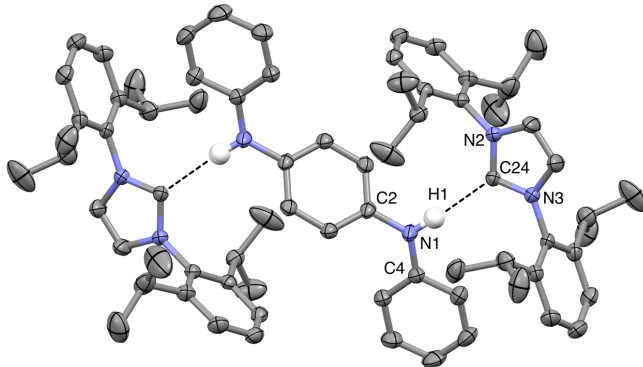


Figure 53. ORTEP diagram of **DPPD···2IPr** adduct (ellipsoids drawn at 50% probability). Non-hydrogen bonding hydrogens have been omitted for clarity. Select bond lengths (Å) and angles (°): H1···C24, 2.30(2); N1···C24, 3.174(2); N2–C13–N3, 101.9(1); N1–H1···C24, 171(2); N2–N3–C4–C2, -17.41(7).

	<b>DPPA···2IPr Adduct</b>
Empirical Formula	$C_{72}H_{88}N_6$
Formula Weight	1037.48
Temperature	100.0 K
Wavelength	1.54178 Å
Crystal System	Monoclinic
Space Group	P 21/n
a	12.2815(2) Å
b	10.7523(3) Å
c	23.4308(4) Å
$\alpha$	90 °
$\beta$	94.3400(10) °
$\gamma$	90 °
Volume	3085.27(11) Å <sup>3</sup>
Z	2
Density (calculated)	1.117 Mg/m <sup>3</sup>
Absorption Coefficient	0.491 mm <sup>-1</sup>
F(000)	1124
Crystal Size	0.29 x 0.26 x 0.23 mm <sup>3</sup>
Theta range for data collection	3.784 to 68.215 °
Index Ranges	-14<=h<=14, -12<=k<=12, -28<=l<=27
Reflections Collected	19666
Independent Reflections	5642 [R(int) = 0.0246]
Completeness to Theta = 67.679 °	99.9 %
Absorption Correction	Semi-empirical from equivalents
Max. and Min. Transmission	0.7531 and 0.6747
Refinement Method	Full-matrix least-squares on F <sup>2</sup>
Data / Restraints / Parameters	5642 / 0 / 384
Goodness-of-fit on F <sup>2</sup>	1.025
Final R Indices [ $>2\sigma(l)$ ]	R1 = 0.0489, wR2 = 0.1226
R indices (all data)	R1 = 0.0599, wR2 = 0.1307
Largest Diff. Peak and Hole	0.360 and -0.347 e.Å <sup>-3</sup>

### CD

During the crystallization of **CD···2IPr** we were able to obtain crystals suitable for X-ray diffraction. The resulting structure was instead of the parent **CD** monomer, with no **IPr** present in the crystal. The unit cell consists of four independent units with slight variability in the central dihedral of the diphenyl moiety (average  $\varphi = \pm 36^\circ$ ). CCDC number: 2011392

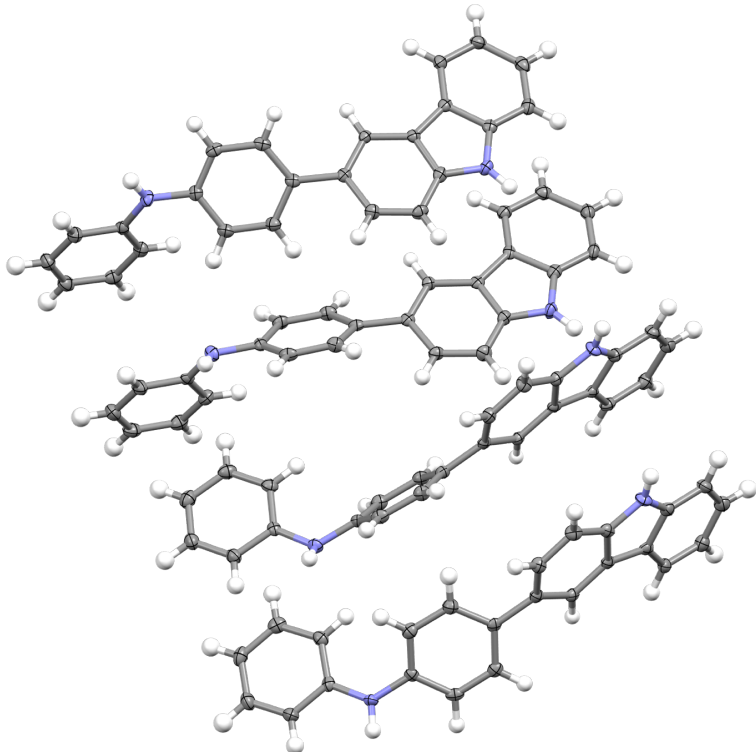


Figure 54. ORTEP diagram of **CD** (ellipsoids drawn at 50% probability) showing four independent units in the unit cell.

	<b>CD</b>
Empirical Formula	C <sub>24</sub> H <sub>18</sub> N <sub>2</sub>
Formula Weight	334.40
Temperature	100.0 K
Wavelength	1.54178 Å
Crystal System	Triclinic
Space Group	P1
a	9.7054(2) Å
b	9.9914(2) Å
c	17.4974(3) Å
$\alpha$	98.0950(10) °
$\beta$	90.7670(10) °
$\gamma$	90.0300(10) °
Volume	1679.67(6) Å <sup>3</sup>
Z	4
Density (calculated)	1.322 Mg/m <sup>3</sup>
Absorption Coefficient	0.599 mm <sup>-1</sup>
F (000)	704
Crystal Size	0.33 x 0.31 0.09 mm <sup>3</sup>
Theta range for data collection	2.551 to 68.389 °
Index Ranges	-11<=h<=10, -12<=k<=12, -21<=l<=21
Reflections Collected	46621
Independent Reflections	11741 [R(int) = 0.0363]
Completeness to Theta = 67.679 °	97.7 %
Absorption Correction	Semi-empirical from equivalents
Max. and Min. Transmission	0.7531 and 0.6665
Refinement Method	Full-matrix least-squares on F <sup>2</sup>

## 6) References

- (1) Arduengo, A. J.; Craig, H. A.; Goerlich, J. R.; Marshall, W. J.; Unverzagt, M. Imidazolylidenes, Imidazolinylidenes and Imidazolidines. *Tetrahedron* 1999, **55**, 14523–14534.
- (2) Mallick, S.; Maddala, S.; Kollimalayan, K.; Venkatakrishnan, P. Oxidative Coupling of Carbazoles: A Substituent-Governed Regioselectivity Profile. *J. Org. Chem.* 2019, **84**, 73–93.
- (3) Paliulis, O.; Ostrauskaite, J.; Gaidelis, V.; Jankauskas, V.; Strohriegl, P. Synthesis of Conjugated Carbazole Trimers and Pentamers by Suzuki Coupling. *Macromol. Chem. Phys.* 2003, **204**, 1706–1712.
- (4) Kim, M.; Jeon, S. K.; Hwang, S. H.; Lee, S. S.; Yu, E.; Lee, J. Y. Correlation of Molecular Structure with Photophysical Properties and Device Performances of Thermally Activated Delayed Fluorescent Emitters. *J. Phys. Chem. C* 2016, **120**, 2485–2493.
- (5) Chu, M.; Scioneaux, A. N.; Hartley, C. S. Solution-Phase Dimerization of an Oblong Shape-Persistent Macrocycle. *J. Org. Chem.* 2014, **79**, 9009–9017.
- (6) Kieser, J. M.; Kinney, Z. J.; Gaffen, J. R.; Evariste, S.; Harrison, A. M.; Rheingold, A. L.; Protasiewicz, J. D. Three Ways Isolable Carbenes Can Modulate Emission of NH-Containing Fluorophores. *J. Am. Chem. Soc.* 2019, **141**, 12055–12063.
- (7) BindFit v0.5 <http://app.supramolecular.org/bindfit/> (accessed Dec, 2019).